Exploratory Research on Crochet: Assessing its Potential as a Fabrication Technique for Soft Robotic Systems and Biomedical Devices

Master's Thesis

Marina Gómez Fernández
s3056953

Faculty of Engineering Technology- Department of Biomechanical Engineering
Soft Robotics Lab

Examination Committee
Supervisor – Prof.dr.ir Herman van der Kooij
Daily Supervisor – Dr. Ali Sadeghi
External member – ir. Edsko Hekman

University of Twente, Enschede, 28/11/2024

UNIVERSITY
OF TWENTE.

oft Robotics Lab

Acknowledgments

Crochet has always been an essential part of my life. I am grateful to the lady who taught me how to crochet a scarf during lunch break. Grateful to my grandma for always keeping the art of crochet alive, and grateful to Ali for translating it from the little blue scarf into a thesis journey.

This thesis has been (mostly) a pleasure from start to finish.
I would like to thank my parents and friends, for attempting (emphasising the word *attempting*) to understand how one thing can relate to another, support, and feedback. And to the lab, for their guidance, question-solving, and for generously assisting as photographers and models during the testing -and mostly re-testing- of prototypes.

Special thanks to Dr. A. Sadeghi, Prof. H. van der Kooij, and ir. E. Hekman for their supervision and expertise.

Abstract

Soft robots benefit significantly from the integration of textiles and fibers in their design and fabrication, serving a wide range of purposes such as defining the robot's behaviour, deformation upon actuation, and capabilities. Among textile fabrication methods, crochet techniques offer a unique approach to exploring the mechanical properties of textiles. By combining different stitch patterns and yarn materials, key parameters such as tensile strength, anisotropy and stiffness can be tuned, providing valuable insights into the fabric's performance.

Additionally, this study addresses the gap in literature and research of crochet in the technical, soft robotic, and biomedical fields. Even though crocheted fabrics have demonstrated to withstand higher loads and deformations than knitted fabrics, no State of the Art considers crochet as a fabrication technique. Nonetheless, knitting has a significant number of publications.

The primary objective of this study is to explore the potential of crochet as a manufacturing technique for creating intricate fiber patterns that enable motion within the realm of soft robotics systems. A comprehensive investigation, classification, and characterization of various crochet patterns is conducted to develop a mechanical understanding, and theoretical model that predicts the behaviour of the resulting structures. An open-source 3D crochet interface is employed to enhance visualization and improve the reproducibility of the structures.

This theoretical framework is applied to demonstrate the innovative use of crochet as a fabrication method for soft robotic systems. Notable examples include a finger-like gripper, a toroidal gripper and locomotion crawling worm. The novelty of this research comes with the design of biomedical devices such as an assistive glove to reduce hand-grasping force and peristaltic valves simulator.

Table of Contents

I. INTRODUCTION

A. Introduction to Soft Robotics

The development of **soft robots** is a rapidly growing interdisciplinary field of study and experimentation. Unlike rigid-body robots, soft robots possess the ability to emulate the movements of the human body and operate in a wider variety of environments. One key advantage of soft robots in the medical field is their ability to distribute forces evenly over larger contact areas, preventing damage caused by high-force concentrations at specific points of contact. This makes soft robots ideal for human interactions as assisting devices [1].

The field of soft robotics is well-versed in the actuation of soft materials. Actuators are mechanical devices designed to induce strain in a system, thereby generating movement or shape change [2]. Soft actuators have played a key role in developing bio inspired artificial systems, such as octopi's arm [3], robotic fish [4], or a tongue [5].

Soft robots in the **biomedical device field** combine their inherent flexibility with the use of biocompatible materials, to achieve biomimicry (i.e., matching the mechanical properties of human tissues) [6]. This latter aspect is a key consideration for compliance matching, which has been successfully demonstrated in various structures, including artificial muscles, muscle alternatives, prosthetic devices, catheters, stents, and surgical instruments [7].

New soft actuators are under development to serve as artificial muscles for patients with facial paralysis [8], as well as to provide grasping capability during neurological rehabilitation [9, 10] (Figures 1a-c). Elastomeric soft robotic ventricular assist devices (VADs) have been developed by Roche et al. to improve heart deficiencies [11] (Figure 1d). Additionally, an electroactive polymer-actuated stent capable of shrinking and expanding via voltage has been developed for nano drug-delivery applications [12]. Conductive polymers are also being employed for ballooning arterial re-opening during percutaneous transluminal coronary angioplasty (PTCA) treatments [13]. The integration of soft-bodied silicone braided sleeve robots into the da Vinci surgical system combines the intuitive control of the da Vinci, with the flexibility of the soft robot [14] (Figure 1e). Furthermore, Luo et al. [15] developed a pneumatically actuated knitted soft hand, able to mimic the opposing thumb movement required to grasp various objects (Figure 1f).
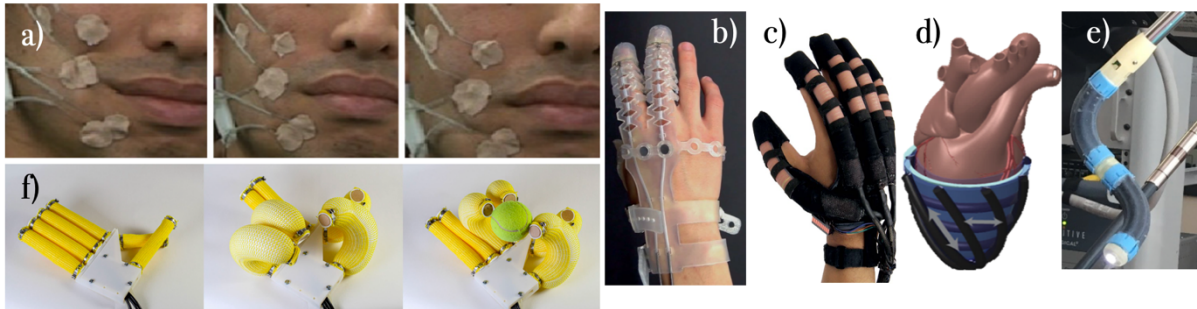

Figure 1. (a) Three different artificial facial expressions generated through Robot Mask [8]. (b) Exo-Glove Poly [9]. (c) Soft Robotic Glove [10]. (d) Elastomeric sleeve to restore the functionality of the heart [11]. (e) Stiffness controllable flexible manipulator for surgical operations [14]. (f) Soft Hand, pneumatic valve system with individual actuation [15].

The use of **pneumatic actuators** for shape-changing motions has been established in several studies [16]. Although these structures show great promise, they are often difficult to fabricate and tend to have rubbery surface characteristics, which may not be suitable for all applications [17]. Pneumatic textile actuators address this issue while still achieving shape changes, induced by an internal bladder being inflated by an external air source. The textile serves as a constraining sleeve material, and its mechanical characteristics will dictate the actuation path and shape upon inflation. By controlling the level of pressure inflow, the overall stiffness of the actuator can be modulated [18]. **Variable-stiffness control** has become a significant topic within soft robotics, especially with the challenge towards rigidity control. While the inherent softness of robots allows for conformational adaptability and resistance to trauma, these properties become disadvantageous when attempting to directly manipulate the environment in which the robot operates [19].

Textiles, being flexible, lightweight, breathable, and relatively strong, are widely used in various daily applications. Textile fabrication processes can incorporate fibers with a lot of variable properties (e.g. stiffness, thermal resistivity, electrical conductivity). Moreover, complex 3D-shaping can be achieved within a single strand of yarn while remaining cost-effective. In this study, we consider crochet as a fabrication method for soft robots, demonstrate example applications, and discuss the design and fabrication parameters to achieve them.

B. Introduction to Crochet

Crochet is a relatively modern 19th century craft, consisting of the manual process of manufacturing fabric with a crochet hook and a single strand of yarn. The hook is used to make specific knot patterns with the yarn, referred to as a stitch. Stitches can be connected to any place within the fabric, allowing the creation of both flat and 3D-shapes [20]. Knitting, often confused with crochet, uses two needles to create stitches, and has been industrially mechanised since 1589 [21]. Figure 2 demonstrates a comparison between a crocheted and a knitted object, whilst using the same pattern it can be highlighted how the crocheted one holds its 3D-form better than the knitted one, which is more malleable [22].

Figure 2. Comparison between a crochet (left) and a knitted (right) object. Same needle and yarn size used [22].
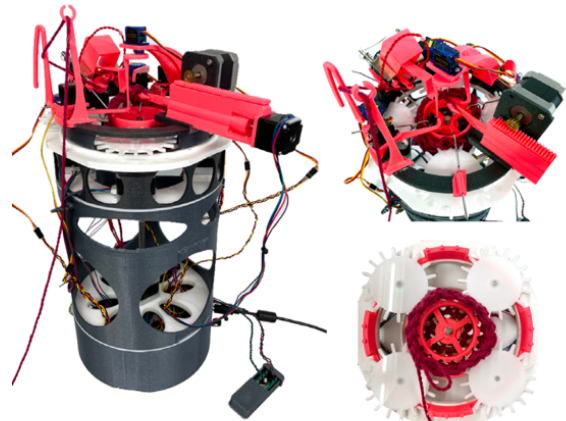

Figure 3. The Croche-Matic robot prototype [28].

Crochet has been applied beyond the realm of crafts. Previous works (Figure 4) have shown how this technique applies to the physical representation of complex mathematical models and theories (e.g., Euclidian and non-Euclidean surfaces such as hyperbolic geometry [23], and the Lorenz manifold [24]). Within the biomedical field, applications include a crocheted scaffold that mimics human skin for tissue engineering [25], sensors for measuring elbow joint flexion [26], and achieving the mechanical properties of human tendons and ligaments [27].

Despite its diverse and complex applications, crochet remains largely a manual craft. To date, no industrial manufacturing machine has been developed to fully automate crochet production. A notable advancement in this area is the **Croche-Matic**, a radial crochet machine developed by Perry et al., Figure 3. It generates 3D cylindrical geometries, and while proven successful, the machine remains in developmental stage. Further research includes building an interface for inputting patterns, producing a 3D object on demand, and adding more advanced stitch patterns [28].

This lack of industrialisation, combined with a relatively scarce knowledge of crocheted fabrics -especially when compared to other textile manufacturing methods- has hindered innovation within the field. The soft robotic field has not yet explored crochet, creating a gap between the technique's craft roots and its technical applications. To lay the groundwork for potential crocheted soft robotic biomedical devices, it is necessary to explore the general tensile properties of crocheted fabrics -swatches-. The mechanics of these swatches depend significantly on the crocheter's technique, but if produced by the same person, they can still be reasonable for investigations.
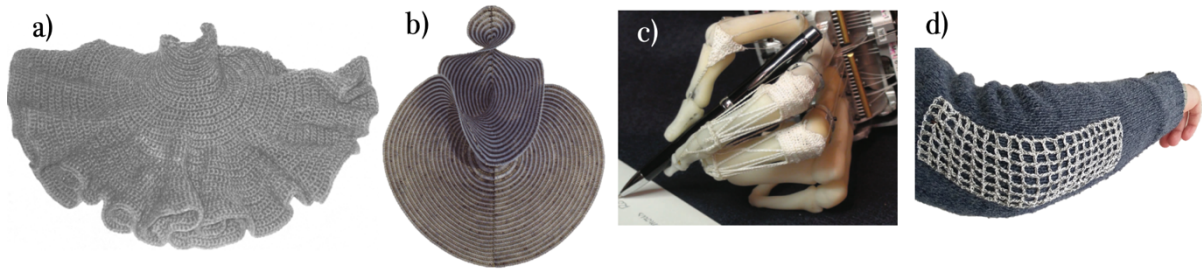
Figure 4. (a) Crocheted annual hyperbolic plane [23]. (b) Crocheted Lorenz Manifold [24]. (c) Crocheted Extensor Hood implemented in the ACT hand [27]. (d) Crocheted piezo-resistive sensor integrated in a sweater [26].

The Technique of Crochet - A stitch is formed by pulling the yarn through tight spaces, resulting in loops wrapped around the hook. The size of the hook influences the tightness of the stitches, and it is usually selected according to the yarn's thickness. Although there are standard stitch types, the possibilities for creating new stitches are unlimited [29].

The basic mechanics of crochet involve three primary stitch-level motions, as illustrated in Figure 5a. The insertion point of the hook is critical in determining the geometry of the resulting stitch; several insertion options are depicted in Figure 5b. Additionally, Figure 5c demonstrates how varying the number of loops on the hook can alter the height of the stitch. These factors–stitch size, number of stitches per row, and the interaction between neighbouring rows–collectively determine how stitches interact to form the desired surface.
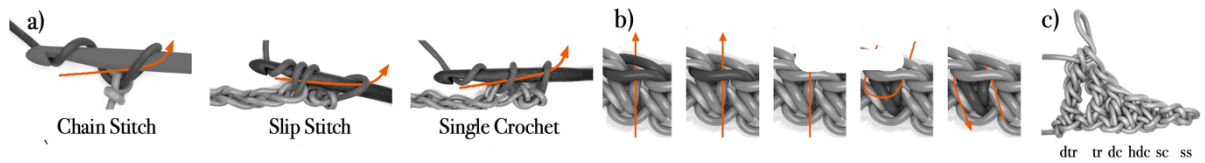

Figure 5. (a) Primary crochet motions and stitches. (b) Insertion points for the crochet hook. (c) Height of common stitches according to the number of loops pulled through the hook [29].

C. State of the Art

Few publications exist where machine knitted, 3D-pneumatically actuated soft robots are simulated and characterised by material, pattern, and motion. Examples include Sanchez et al. [30], Singal et al. [31], and Luo et al. [32]. All these studies employ tensile testing experiments to characterise the extension and apply it accordingly to form actuators with various motions. Singal et al. additionally develop a numerically simulated model using FEM analysis to predict the elastic response of the fabric according to the topology of knitted stitches (Figure 6a, 6b). Other studies propose several approaches for mathematically modelling knitted textiles [33]. Although these methods have proven successful from a stitch-based perspective, knitted stitches follow symmetrical patterns that crocheted stitches do not exhibit, such a broader range of stitch-to-stitch interactions and shapes. This difference makes the mathematical basis for modelling crocheted structures more intricate and less straightforward. Storck et al. [34] developed a topology-based model using Python and Text Mind, suitable for FEM applications, to study the mechanical properties of crochet (Figure 6c, 6d).
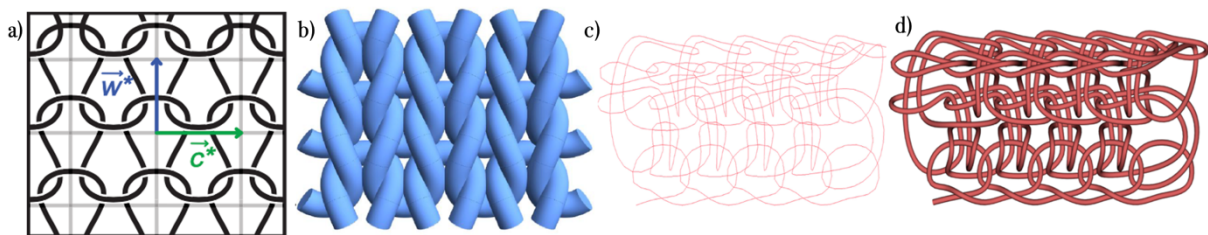

Figure 6. (a) Knitted yarn path, basis for the mathematical modelling [33]. (b) TexMind Viewer of a knitted fabric following the yarn path in (a) [31]. (c) FEM Model generated from the mathematical model of crocheted fabrics [34]. (d) TexMind viewer of a crocheted fabric [34]

Storck et al [35] also characterised both knitted and crocheted fabrics by conducting tensile tests. Results showed that crochet was able to withstand higher loads at larger elongations than knitted fabrics as shown in Figure 7. Which suggests that crochet is suitable for applications requiring higher mechanical stability, while also offering the capability to create complex 3D structures. These findings highlight the need for further research into crochet as a technical textile.
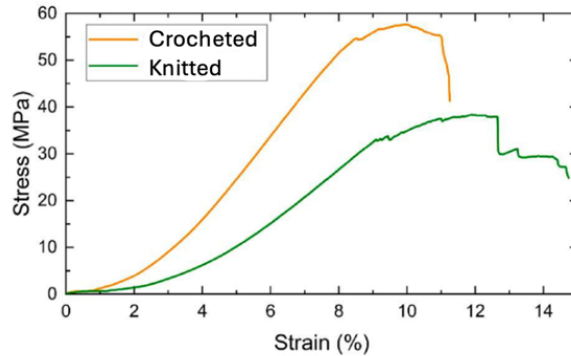

Figure 7. Stress-strain curves of Crocheted and Knitted fabrics [35].

A mechanical model considers both the elasticity of the yarn and the topology of the stitch, which are important contributors for modulating the stiffness of the resulting crocheted 3D structure. When the crocheted swatch undergoes deformation, each element contributes accordingly. To characterise this, several swatches of consistent size but with different stitch pattern were crocheted. Tensile testing experiments were then conducted to measure the mechanical response of the fabric whilst monitoring changes in the swatch's shape.

D. Objectives and Research Question

This study aims to explore crochet as a fabrication method for developing structures that can simulate movements commonly observed in soft robotic systems. Once basic motions can be achieved and characterised, the second objective is to design and crochet several biomedical device's prototypes. To reach these goals, it is necessary to first conduct an investigation and characterisation of crocheted fabrics. This third objective serves as the foundation for understanding how varying fundamental crochet parameters, such as stitch pattern and yarn material, influences the mechanical properties of the swatch. These properties will dictate the actuation path, and functional capabilities of the resulting 3D soft robotic structure. The arisen research questions can be formulated as: How does the combination of stitch pattern and yarn material dictate the mechanical properties of the crocheted structure? Is there a way to predict the behaviour of the fabric to tune the stiffness of the resulting soft robotic structure?

II. METHODOLOGY

A. The Modelling of Textiles

The modelling of textiles can be done at different scales. Firstly, the macro-scale, where the textile structure is represented as a continuum plate with a given mechanical behaviour. Secondly, the meso-scale where the textile is divided in unit cells, with each cell representing the yarn path as a geometrically intermeshed structure. Finally, the micro-scale considers the fiber-to-fiber interactions within the yarn [36].

In this study, macro-scale approach will be adopted to model a selection of crochet patterns by conducting a series of uniaxial tensile testing experiments. Their overall mechanical response, in combination with intrinsic yarn parameters such as cross-sectional area and elastic modulus, will be used to define a set of parameters and their contributions to each of the patterns.

Once these parameters are well-defined, each individual crochet stitch can be considered equivalent to a unit cell, complete with its own yarn path, thus entering the meso-scale modelling phase.

The yarn path of each crochet stitch is illustrated in Figure 8. The defining parameters include the distance between stitches within a row (D) and the stitch height (H).

These values are directly influenced by the yarn diameter, hook size, and stitch pattern. The depth of the stitch is not considered, as it remains consistent across patterns.

H is further divided in two sections: *L1* and *L2*. This division is based on observations during uniaxial testing, where certain stitch patterns exhibit a larger dominant section (*L1*), while the other section remains relatively constant (*L2*). This behaviour is defined as the strain, or

$$\frac{stitch_a - stitch_b}{stitch_b} = \frac{(l1_a + l2_a) - (l1_b + l2_b)}{l1_b + l2_b}$$

Eq. 1 values are further discussed in *Section 3, Table 3.*

The approach used is a topology-based model, which does not describe the exact curvature between yarn segments, but rather focuses on their general orientation. This simplification facilitates the broader application of the model, making it adaptable to yarns with varying mechanical properties.
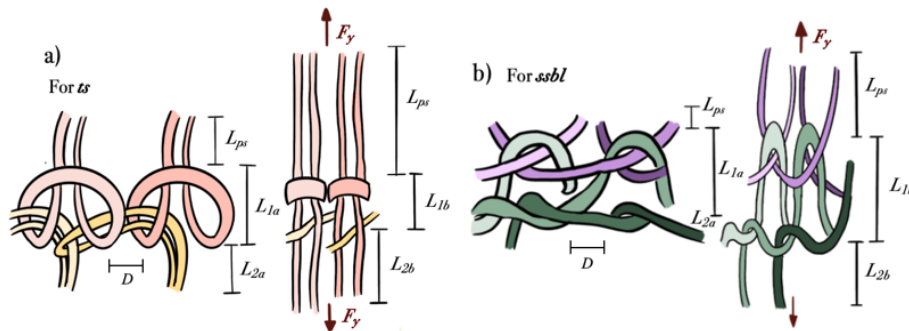

Figure 8. Yarn path and unit cell for: (a) ts stich pattern and (b) ssbl stitch pattern. Non-extended (left) and extended (right). Length of the previous stitch (L_{ps}), H (divided in L_1 and L_2, before and after extension), and D are depicted.

B. Materials and Fabrication

In this study, six different yarn types were used. Of these, three were selected for testing and analysis (Figure 9b). 100% acrylic yarn, 1.5mm in diameter, crochet hook size 3.5mm, purple in colour: *Fama, Lanas Katia,* Spain. 100% Tactel polyamide (i.e. a modified form of nylon), 2mm in diameter, hook size 3mm, green in colour: *Stretchy*, *LM Lanas,* Spain. 100% cotton yarn, 2.5mm in diameter, hook size 4.5mm, blue in colour: *United Cotton, Lanas Katia,* Spain.

For the prototypes applications thinner yarns were also used, 100% cotton, 1.5mm in diameter, crochet hook size 3mm, red in colour: *100% cotton 8/4, Søstrene Grene,* Denmark. 100% mercerized cotton, 1mm in diameter, crochet hook size 1.5mm, green in colour: *Mega Import Thread*, USA. 50% polyester, 50% rubber threads, 1mm in diameter, crochet hook size 1.75mm, black in colour: *Para Cord Elastic,* USA.

Additionally, five different crochet stitch patterns were employed, each selected based on different parameters such as stretchability, stitch size, stitch-to-stitch gap, and stitch topology. Figure 10 illustrates each crochet pattern and main characteristics.

In total, 15 swatches were crocheted -one per yarn and stitch pattern- (Figure 9a). Table 1 details the measurements of each swatch. To validate the mechanical model, an additional six swatches were crocheted. Table 2 provides the measurements and characteristics of these.
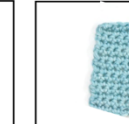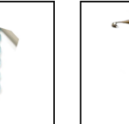

Figure 10. Comparative table of the crochet patterns used in the study, and main characteristics.
Picture source: www.thesprucecrafts.com
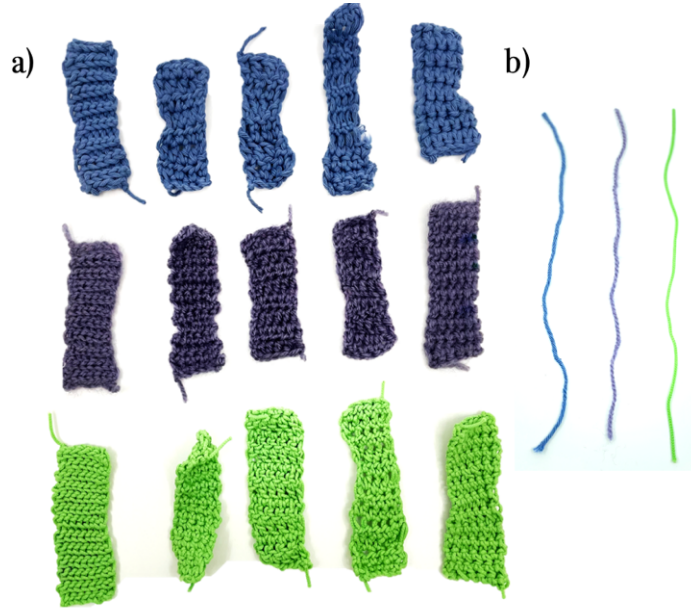
Figure 9. (a) Crocheted swatches: ssbl, sc, hdc, dc, ts (from left to right) and cotton, acrylic, and polyamide yarn (from top to bottom). (b) Tested yarn 65mm samples, cotton, acrylic, and polyamide (from left to right).

TABLE I. DATA MEASUREMENTS OF THE TESTING SWATCHES (IN CM)

Yarn Material	Pattern									
	dc		hdc		sc		ssbl		ts	
	H	L	H	L	H	L	H	L	H	L
Acrylic	7.6	3.4	7.7	3	8	3.1	7.3	3.1	8.4	3.2
Cotton	8.5	3	7.8	3.2	7.8	3.4	8	3.2	7	3.5
Polyamide	8.7	3	8.5	2.7	8.1	2.7	7.5	3	8.1	3

| Yarn Material	Pattern									
	dc		hdc		sc		ssbl		ts	
	H	L	H	L	H	L	H	L	H	L
Acrylic	7.6	3.4	7.7	3	8	3.1	7.3	3.1	8.4	3.2
Cotton	8.5	3	7.8	3.2	7.8	3.4	8	3.2	7	3.5
Polyamide	8.7	3	8.5	2.7	8.1	2.7	7.5	3	8.1	3

TABLE II. DATA MEASUREMENTS OF THE VALIDATION SWATCHES (IN CM)

Yarn Material	Pattern			
	ssbl		ts	
	H	L	H	L
Acrylic	7.6	3.7	8.3	4
Cotton	7.8	3.7	8.7	4.2
Polyamide	7.8	3.9	9	4.4

C. Tensile Testing Experiments

The experiments were conducted using a uniaxial test method, where the force is applied in a single direction. A method suitable for assessing the anisotropic tensile properties of textiles. Tensile testing is a widely used technique for characterising materials in industry and research. The material's internal behaviour is reflected in the tensile test curve, displaying the relationship between load and elongation [36].

The tests were performed with an Instron *Universal Testing Machine (UTM) Model 3343* [37], equipped with clamps designed to prevent lateral and torsional motion. For each sample a section of the swatch was clamped at both ends. Although many experimental studies assess deformation until breakage, the swatches were only tested up to a maximum load of 30N, at a rate of 1mm/sec, approximating a quasistatic regime. Thus, stretching from a relaxed configuration to maximum extension over 1-5 minutes. An initial 'preconditioning' round was performed for each swatch to break apart any fiber connections and detect potential slippage. The data from this round was excluded from the analysis. Between successive testing runs, the swatches were reset to their initial length and briefly stretched in the transverse direction to reconfigure the stitches. All tests were conducted along the y-axis. The pre- and post- extension length was measured using a digital calliper, setup can be seen in Figure 11.

The experimental procedure and analysis were repeated for each of the three yarn samples. In this case, the deformation was assessed until breakage, with an extension rate of 0.5mm/sec. The length of the samples was 95mm.
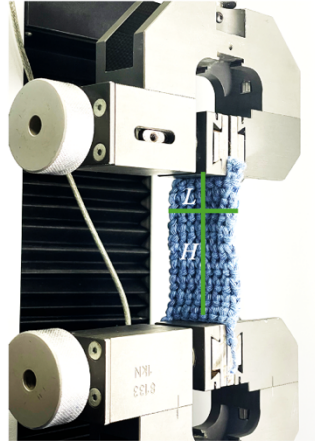
Figure 11. INSTRON 3343 Experimental Setup for all the Tensile Test Experiments

III. RESULTS AND DATA ANALYSIS

The average values used for the analysis are presented in *Section 2, Table 1*: height 70mm, length 31mm, thickness 4.8mm. The strain

$$Strain = \frac{Extension}{Height}$$

and engineering stress values (i.e., the cross-sectional area is considered constant pre- and post-extension)

$$Stress = \frac{Load}{csArea}$$

were calculated. Figure 12 shows the stress-strain curves for different yarn compositions and stitch patterns (abbreviated according to Figure 10).
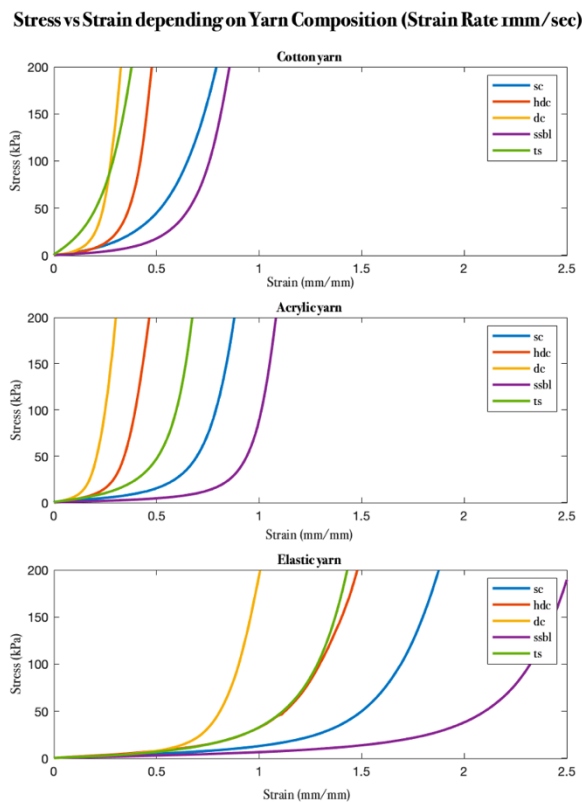
Figure 12. Engineering Stress (kPa) vs Tensile Strain (mm/mm) depending on the yarn material for all five stitch patterns.

Figure 13 depicts the stress-strain curves with hysteresis (i.e., extension and relaxation) for each stitch pattern and yarn material.

For better visualisation, Figure 14 illustrates the strain of each stitch pattern and yarn composition in a stacked bar plot.
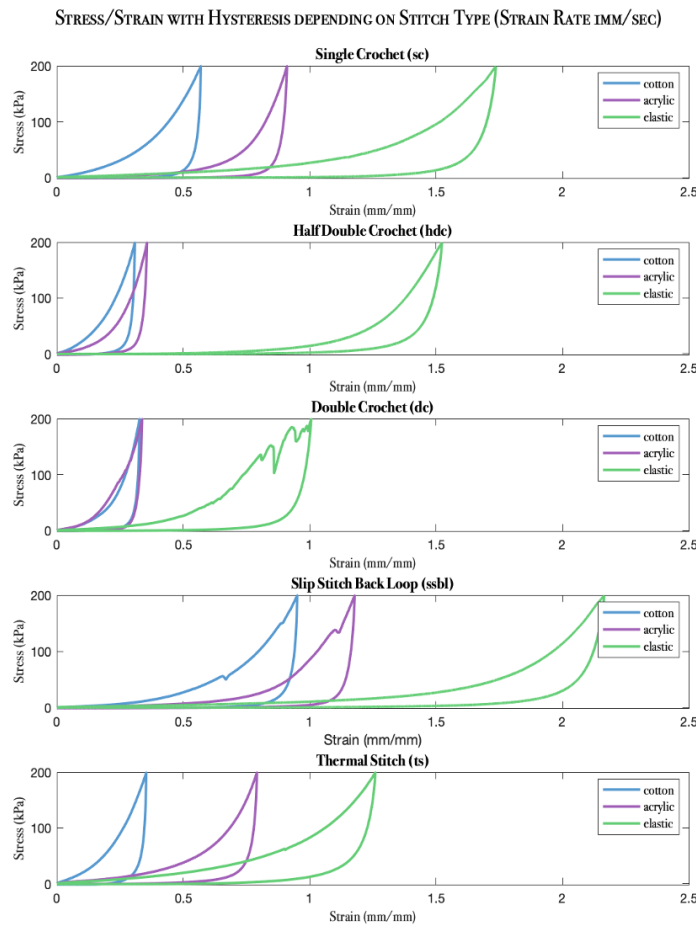
Figure 13. Engineering Stress (kPa) vs Tensile Strain (mm/mm) with hysteresis depending on the stitch pattern for all three yarn materials.

When stretched, the swatches exhibit two distinct mechanical regimes [38].

1. Crochet architecture-dominated regime: In the initial phase, each stitch reconfigures geometrically as yarn slides and straightens to reduce internal stresses, leading to an approximately linear stiffness.

2. Material-dominated regime: Once the yarn can no longer slide further -the reconfiguration inside the stitch is complete-, both the stitches and the yarn itself deform. At this point, the mechanical properties of the yarn govern the behaviour, creating the characteristic J-shaped stress-strain curve.

Due to the viscoelastic nature of the yarns, residual strain is observed in hysteresis.

For further analysis and final applications, two stitch patterns were selected: *Thermal Stitch (ts)* and *Slip Stitch Back Loop (ssbl)* (i.e., the most and least stiff stitch respectively).

Figure 15 shows a comparison between the initial and final elongation of *ts* and *ssbl* patterns for all three yarns. The full motion can be seen in Movie 1, *Supplementary information.*
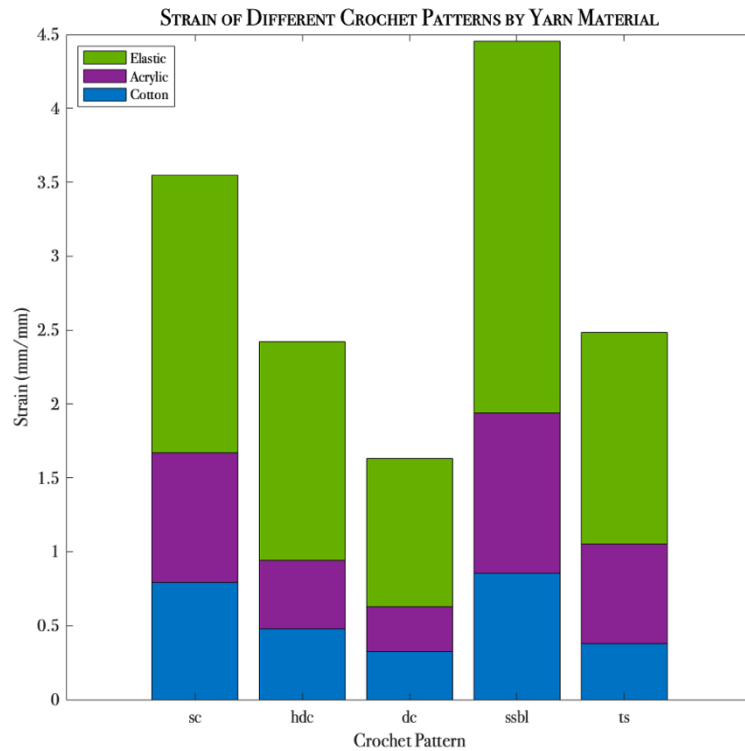
Figure 14. Stacked Bar Plot of Tensile strain (mm/mm) for each of the five patterns.
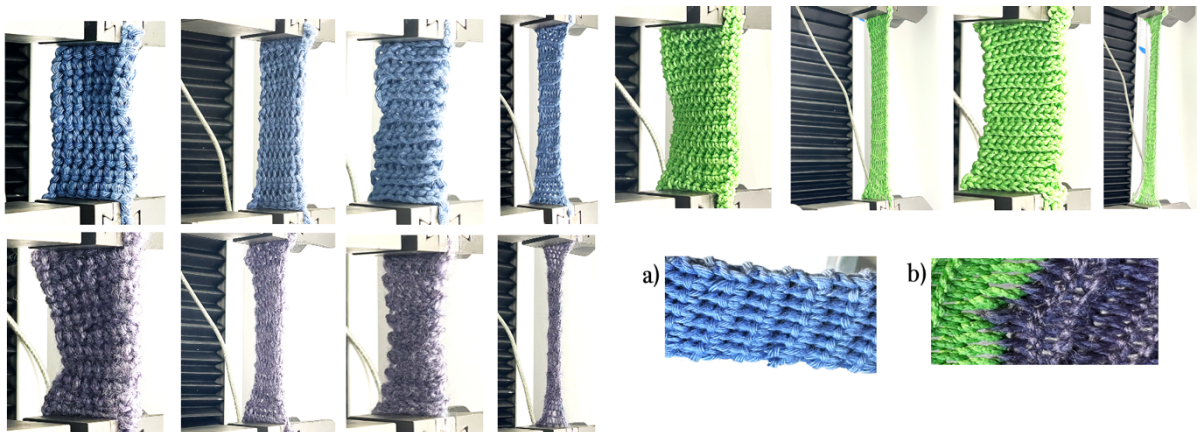
Figure 15. Comparison between initial and final elongation (at 30N). From top to bottom: cotton, acrylic, and elastic yarn. From left to right: ts, and ssbl stitch pattern. (a) and (b) are zoomed in of cotton ts, and acrylic and elastic ssbl.

To gain deeper insight on the role that each individual crochet stitch plays in the stress-strain relationship, the swatches were retested at different lengths -meaning fewer rows of crochet were included in each tensile test-. The selected row counts were 3, 5, 7, and the full swatch. As the yarn diameter and stitch pattern varied, the same number of rows did not always correspond to the same swatch length. The experimental procedure and analysis were repeated for each selected row, with an extension rate was of 0.5mm/sec and 0.27mm/sec for long and short rows respectively. Results can be seen in Figure 16.

Aside from minor discrepancies within the elastic yarn, the number of rows under extension did not significantly affect the stress-strain curves across stitch pattern and yarn material. This result provides a more robust path for assessing the stiffness, defined as the deformation resisted by an object in response to an applied force [39].
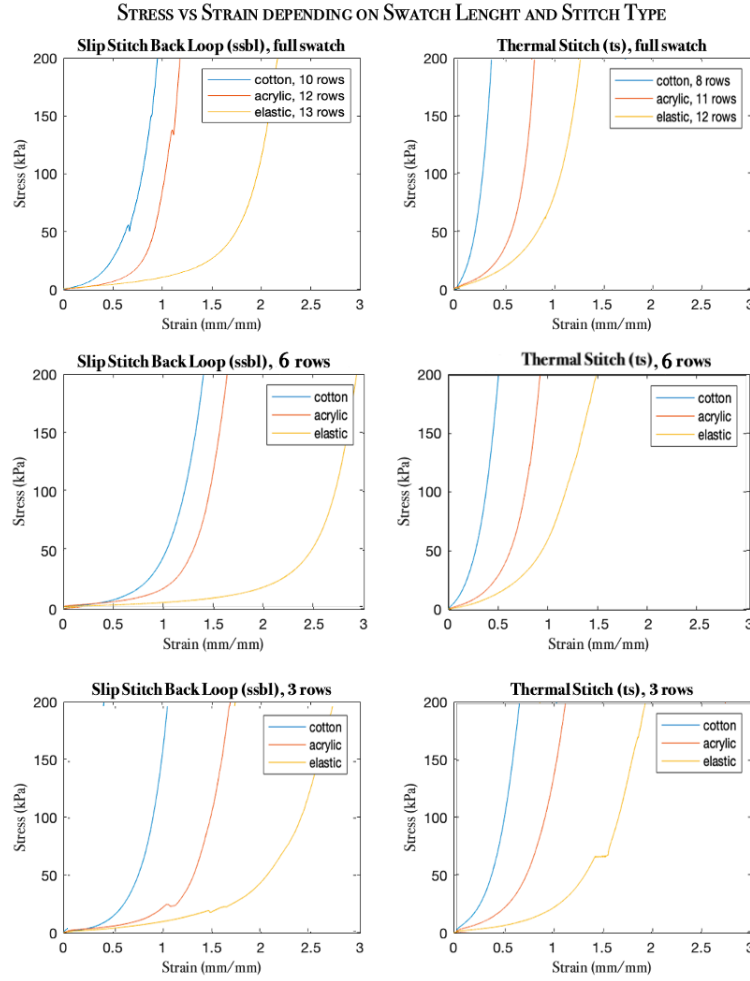
Figure 16. Engineering Stress (kPa) vs Tensile Strain (mm/mm) depending on the number of extended rows in the swatch (full, 6, and 3 rows) and stitch pattern.

To compute the stiffness, the derivative of the fitted exponential load–extension curve was taken, following

$$k(x) = \frac{d}{dx} * f(x), where\ f(x) = ae^{bx}$$

MATLAB was used to fit the exponential curve and calculate the final values. Figure 17 depicts the stiffness against extension for different yarn materials and stitch patterns. Cotton yarn exhibited the highest stiffness across most stitch patterns, showing non-linear behaviour at higher extensions for *dc*, *hdc*, and *ts*.

Acrylic yarn also demonstrated stiffness in two patterns, whilst *ssbl* showed the least, extending to 90mm with a stiffness of 2N/mm. Elastic yarn had the most extensible patterns, with *ssbl* extending up to 170mm (i.e., almost three times the original size) with a stiffness of 1N/mm.

Across all yarn types, *ssbl* consistently showed the lowest stiffness, making it ideal for applications where flexibility and elasticity are prioritized, without significant resistance to deformation. In contrast, *ts* exhibited the greatest stiffness across all yarn materials while presenting the least gaps in between stitches when extended (as depicted in Figure 15b), making it suitable for applications requiring durability and shape retention. Those two stitch patterns, *ts* for cotton yarn and *ssbl* for acrylic and elastic, constitute the basis of the final prototypes. This choice is also corroborated when looking at the strain values for each pattern and material, calculated using Eq. 1, and displayed in Table 3. l_{1b}, l_{2b}, l_{1a} *and* l_{2a} are stipulated in Section 2. The lowest strain was recorded for *ts* cotton, and the highest for *ssbl* elastic.
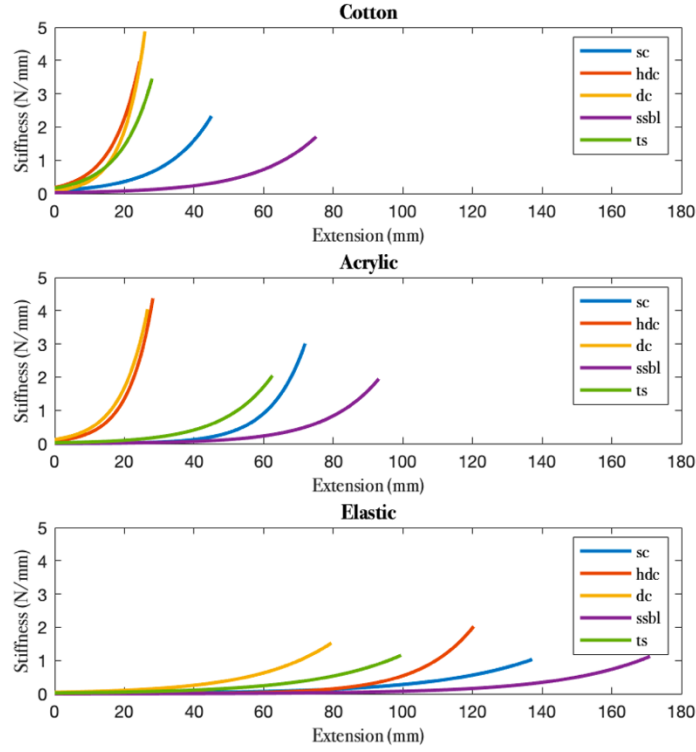
Figure 17. Stiffness (N/mm) vs Extension (mm) depending on the yarn composition and stitch pattern.

TABLE III.   STRAIN MEASURMENTS FOR EACH PATTERN AND MATERIAL (IN CM)

Strain	Yarn and Pattern					
	Cotton		Acrylic		Polyamide	
	ssbl	*ts*	*ssbl*	*ts*	*ssbl*	*ts*
$l_{1b}+l_{2b}$	7	11	5	8.6	5	7.6
$l_{1a}+l_{2a}$	22.2	14.2	16.3	13	25.3	16.9
Strain	2.17	0.29	2.25	0.51	4.05	1.2

Changing the yarn material shifts the transition points between the mechanical regimes, allowing material-based stiffness tunning. Yarns with lower stiffness (i.e., those that are already stretchable in the pre-crocheted state) exhibit different mechanical behaviours when incorporated into crochet patterns. [39]

Figure 18 illustrates the stress-strain curve of each of the three yarns- cotton, acrylic and elastic-. The maximum load supported before failure was of 32, 27, and 60N respectively.

The curve shows four distinct regions: *toe region* representing the alignment of the fibers within the yarn, *linear region*, where all fibers are out of their crimped state and respond to the load linearly. *Plastic region* represents the beginning of the accumulation of microdamage until *failure* (i.e., breakage) is reached [40].

The elastic modulus, -a measure of a material's resistance to elastic deformation- is independent on the geometry of the swatch (i.e. crochet stitch pattern) [41]. Thus, it is only evaluated based on the yarn material. Using a polynomial curve fitter in MATLAB,

$$f(x) = p_1 x + p_2$$

the elastic moduli were determined to be 4.5 MPa for cotton, 2.6 MPa for acrylic, and 1.2 MPa for elastic yarn. Figure 19 shows the stress-strain curves for each yarn, with non-linear regions excluded in red.

11

MEAN STRESS VS STRAIN CURVES WITH STANDARD DEVIATION FOR YARN MATERIALS
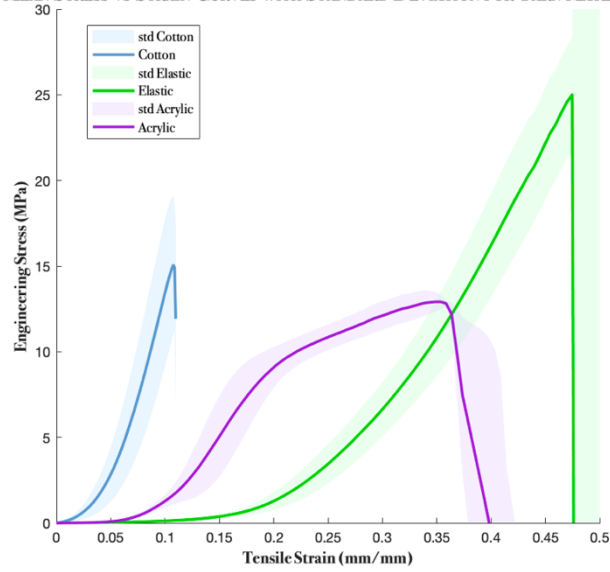
Figure 18. Mean Engineering Stress (MPa) vs Mean Tensile Strain (mm/mm) for Cotton, Acrylic, and Elastic yarn. Tested until breakage, Strain Rate 0.5mm/sec.

ELASTIC MODULUS CURVE FITTER FOR COTTON YARN
ELASTIC MODULUS CURVE FITTER FOR ACRYLIC YARN
ELASTIC MODULUS CURVE FITTER FOR ELASTIC YARN
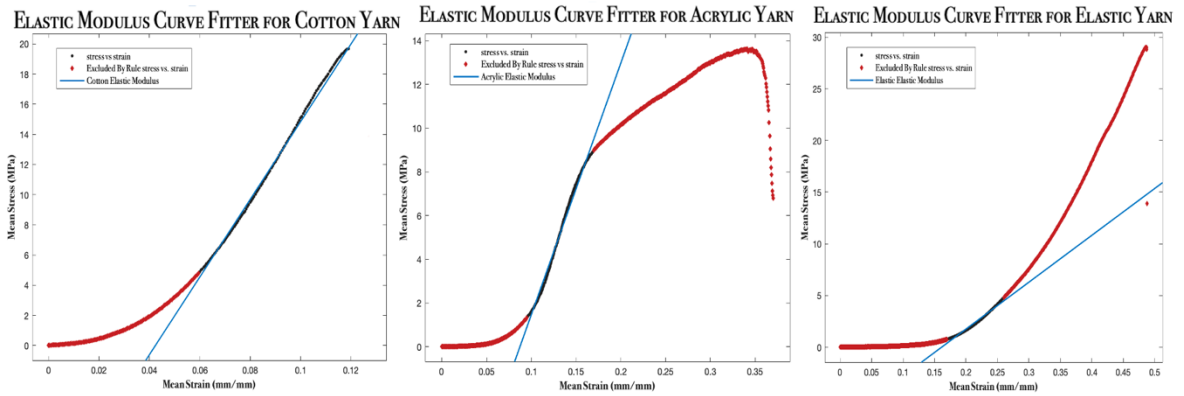
Figure 19. Curve Fitting of the mean value Engineering Stress (MPa) vs Tensile Strain (mm/mm) to obtain the Elastic Modulus of each yarn material. From left to right: cotton, acrylic and elastic yarn.

In conclusion, by analysing the stress-strain profiles, stiffness, and strain values, this study identified that *ts* for cotton, and *ssbl* for acrylic and elastic yarn provide the contrasting mechanical properties required for the targeted soft robotic applications. This characterisation forms the basis for material selection, ensuring the optimal balance for flexibility and stiffness upon actuation.

IV. Modelling the Stiffness Behaviour of Crochet with a Topology-Based Mechanical Model

To modulate the stiffness of 3D crochet structures, each stitch will be modelled as a spring of stiffness k. In a row of n crochet stitches there will be n different *k-values* in parallel. The main contributors to stiffness modulation are the stitching pattern and the yarn material. We experiment with two different patterns, *ts* for extensible and *ssbl* for non-extensible behaviour. Additionally, we use three different yarn materials -cotton, acrylic and elastic- each with distinct elastic moduli.

When a force -extension-, is applied along the y-axis (F_y) each spring will undergo a strain, defined as the deformation per unit length [41]

$$\epsilon = \frac{\Delta L}{L}$$

The strain value depends on the material properties and stitch pattern's geometry, but not on the length (as illustrated in Figure 16). Each spring within the same row, k_i, will experience the same strains -the deformation of each crochet stitch in the same row is equal-, and different stresses [42]. Thus, k_i undergoes the same stiffness across the row. An illustration of the model's basis can be seen in Figure 20.
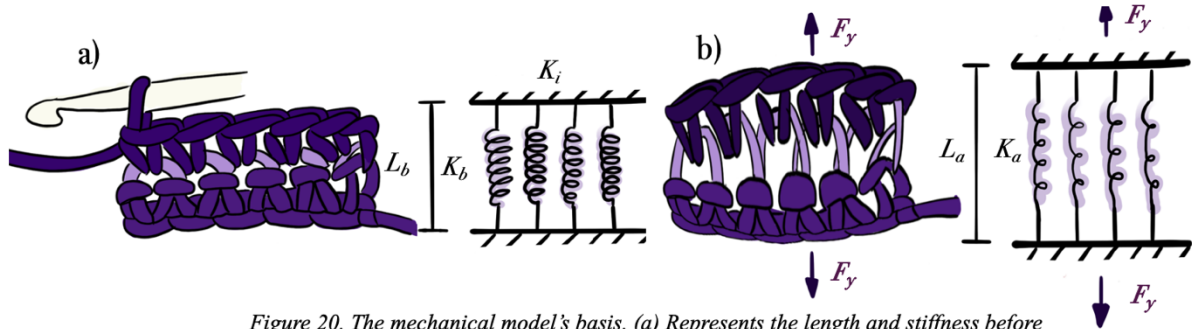
Figure 20. The mechanical model's basis. (a) Represents the length and stiffness before extension (Fy). (b) Representations after extension.

By following

$$K = \frac{E * csA}{L}$$

we assume that the cross-sectional area (csA) remains constant for all samples, E is an intrinsic property of the yarn, and L changes and we modify the number of rows under extension. As the number of rows (L) increases, the maximum stiffness value decreases, forming a linear relationship.

By interpolating different data points, the behaviour of the stiffness curve can be predicted for new conditions (Figure 21). For a single row of crochet, since the stiffness is uniform, the value of each individual stitch can be known.

Eq. 7 is obtained by combining Eq. 6 and Hooke's Law, relating force, stiffness, and deformation

$$F = \frac{k}{\Delta L}$$

Stress is related to strain through the elastic modulus

$$\sigma = E * \epsilon$$

and defined as

$$\sigma = \frac{F}{A}$$

This shows that stiffness and strain are inversely proportional, as seen in Figure 21.

To compute the stiffness ratio (K_r), K is normalised over L, enabling a consistent basis for comparing different configurations of crochet rows and stitch patterns. K is also influenced by E, therefore by dividing by this factor, we remove the influence of the material properties as well

$$k_r = \frac{K * L}{E}$$
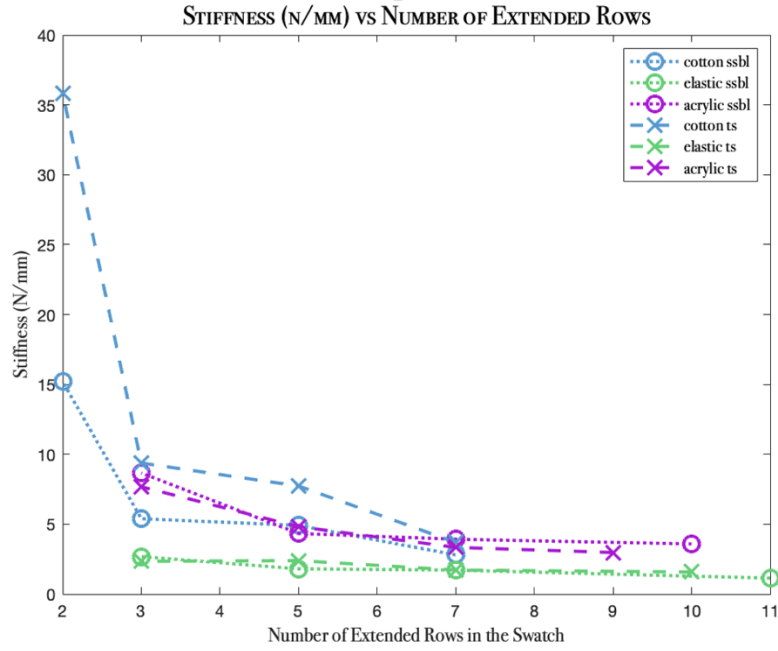
Figure 21. Stiffness (N/mm) vs the Number of Extended Rows in the Swatch. For Cotton: 2,3,5 and 7 rows. For Acrylic: 3,5, 7, and 9 (ts) or 10 (ssbl) rows. And for Elastic: 3,5,7, and 10 (ts) or 11 (ssbl) rows.

This ratio remains constant within a range for the same stitch pattern and yarn material, regardless of the number of extended rows (*L*). Results are displayed in Table 4. The mean value is computed per each combination of pattern and material. This stability makes K_r useful for analysing and predicting the behaviour of crochet swatches, isolating the intrinsic characteristics of the stitch pattern and yarn material.

TABLE IV.   STIFFNESS RATIOS FOR EACH PATTERN AND YARN.

Stiffness Ratio	Yarn and Pattern					
	Cotton		*Acrylic*		*Polyamide*	
	ssbl	*ts*	*ssbl*	*ts*	*ssbl*	*ts*
Full Swatch	39.5	68.2	68.3	77.4	67.9	84.3
7 Rows	36.2	69.6	60.8	71.7	65.2	76.1
5 Rows	38.8	67.5	41.6	61.6	43.5	74.3
3 Rows	27.1	61.7	34.5	50.2	35.1	47.6
Average K$_r$	**35.4**	**66.7**	**51.3**	**65.2**	**52.9**	**70.6**

A first approximation to predict the stiffness of a given pattern and yarn for any length is

$$K_p = \frac{K_r * E}{L}$$

No mathematical way to predict the contribution of each variable (i.e. material and pattern) was successfully reached. Therefore, the approach taken is to predict contributions by assessing the plots. Figure 12 shows that the pattern-selection has a greater impact on the behaviour of the curve than the material-selection.
  -For cotton and acrylic yarn, the contribution is assumed to be 65% pattern /35% yarn.
  -For elastic yarn, the contribution is assumed to be a 60% pattern /40% yarn.

Eq. 12 now rewrites as $$K_{predicted} = \frac{(C_{material} + C_{pattern}) * E}{L}$$

$C_{material}$ and $C_{pattern}$ are specified in Table 5.

14

TABLE V.   CONSTANTS FOR EACH YARN AND PATTERN.

Stiffness Constant	Yarn and Pattern					
	Cotton		Acrylic		Polyamide	
	ssbl	ts	ssbl	ts	ssbl	ts
$C_{material}$	15	15	20	20	25	25
$C_{pattern}$	20.4	51.8	31.3	45.2	27.9	45.6

A. Testing

The model was tested using swatches of varying lengths (full, 7, 5, and 3 rows). Table 1, *Supplementary Information,* shows both the predicted stiffness results and the actual stiffness values computed using MATLAB, following *Eq. 4* and *Eq. 14* respectively. Figure 22 deploys the table in a bar plot for better interpretation of the result's proximity.

Figure 22. Predicted (in blue) vs MATLAB (in orange) Stiffness (N/mm) bar plot to assess the accuracy of the testing of the mechanical model. Written above the bars the length of the swatch. and below the yarn material and pattern.

B. Validation

The model was validated using two different sets of data:
1.   The original swatches, tested for three lengths (6, 4, and 1 row).
2.   The validation swatches with a higher number of stitches per row than the originals, tested at full length.
Results are displayed in Table 2, *Supplementary Information.* Figure 23 deploys the table in a bar plot.

A final consideration was the force applied during the tensile test experiments, which was set at a final extension of 30N. Stiffness may behave differently when lower forces are applied. Figure 24 illustrates load versus extension, showing extensibility's saturation point for each yarn material. Above 10N, a plateau (i.e. extension increases very slowly under additional load) occurs for cotton and acrylic yarn, while for elastic yarn the behaviour occurs at 15N.
Figure 25 shows the linearity of stiffness against load for three swatches at maximum extension loads of 30N and 15N.
The maximum stiffness at 15N is approximately half of the value at 30N, allowing for an easy calculation when predicting the stiffness under a different extension load.

This assumption is validated in Table 2, *Supplementary Information* for both the original swatches and the validation ones.
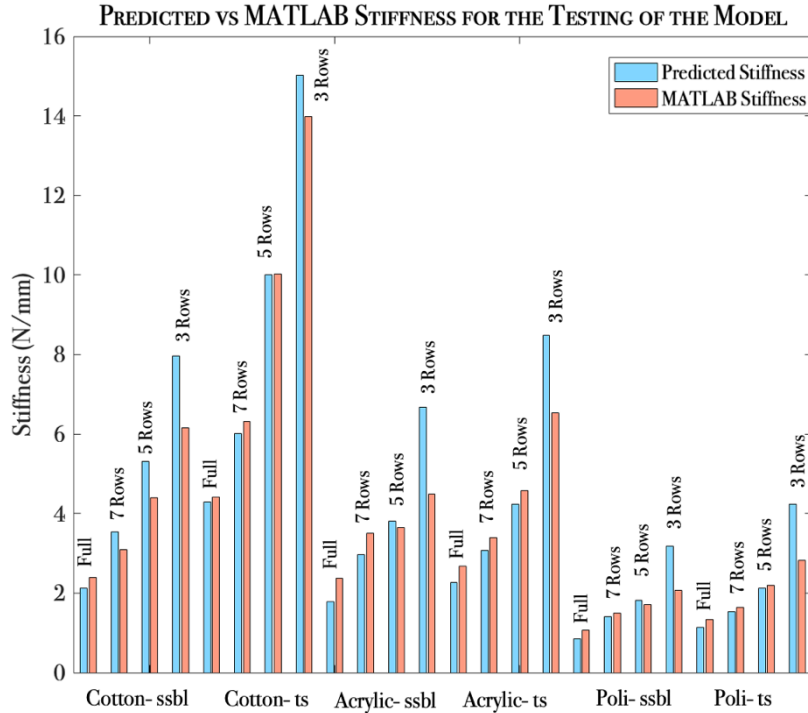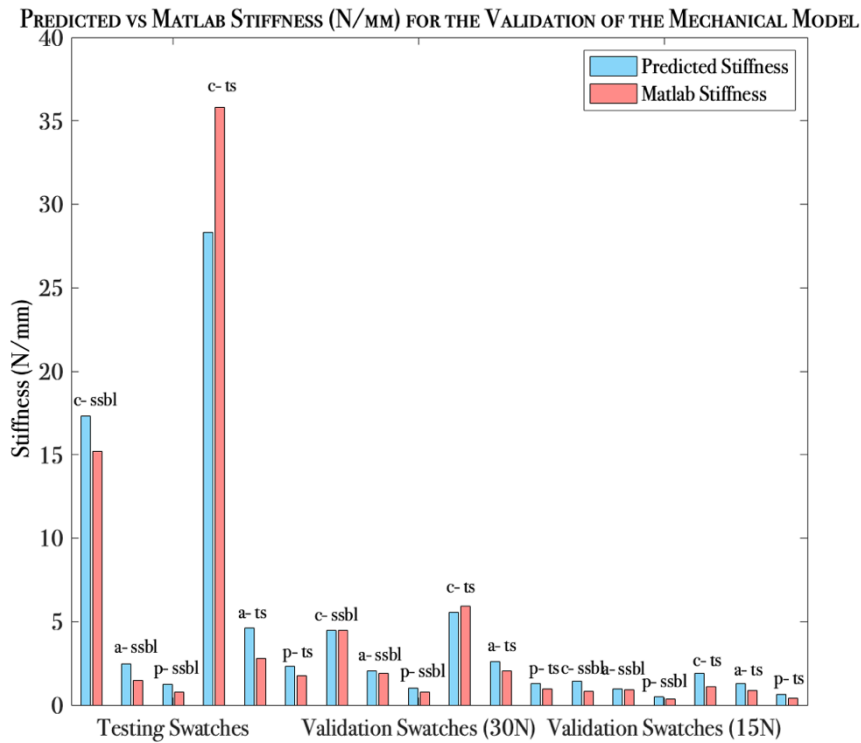

Figure 23. Predicted (in blue) vs MATLAB (in orange) Stiffness (N/mm) bar plot to assess the accuracy of the validation of the mechanical model. Written above the yarn material (c, a, p for cotton, acrylic, and polyamide respectively) and pattern.
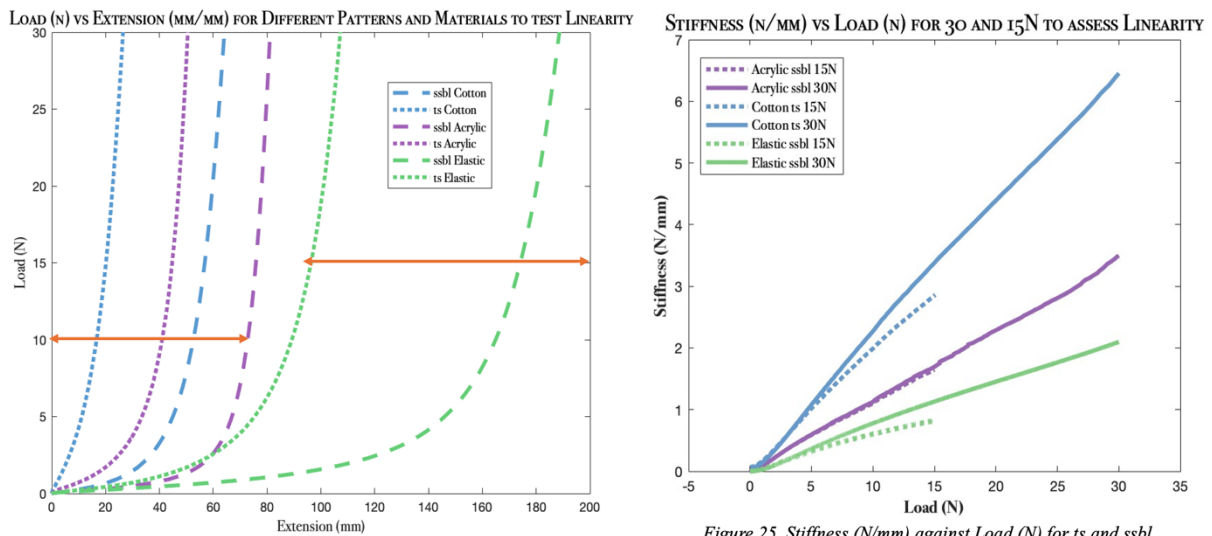
Figure 24. Load (N) vs Extension (mm) for two stitch patters and all yarn materials to observe at which load the plateau behaviour starts.

Figure 25. Stiffness (N/mm) against Load (N) for ts and ssbl pattern and all yarn materials. Tested under 30 and 15N to assess stiffness linearity for both extension loads.

The model validation results are consistent, *ssbl* shows better results than *ts*. This is likely due to the higher complexity of the stitch's geometry of the later one. Elastic yarn predictions are the closest to the real values, indicating a good understanding of the material's behaviour in the model.

Once the results are validated, the stiffness for a single stitch can be predicted, as deployed in Table 6. These values are in alignment with the conclusions from the tensile tests and open the door for future studies to select a stitch pattern and yarn, based on the desired outcome stiffness. This tunability will allow for the achievement of different motions or extensibilities within the realm of soft robotic systems, as it will be explained in the following section.

Stiffness (N/mm)	Yarn and Pattern					
	Cotton		Acrylic		Polyamide	
	ssbl	*ts*	*ssbl*	*ts*	*ssbl*	*ts*
	16	30	18	23	10	13

V. PROTOTYPE FABRICATION METHOD

The actuator's ability to achieve desired deformations depends on the variability in extensibility provided by the crocheted structures -stitch pattern and yarn material-. We fabricated multiple crochet-based structures to characterize the bending performance of actuators under these defined variables. The actuator is divided within the front and back panel. The front panel is composed of 75% acrylic yarn in *ssbl* -extensible- pattern (purple in colour), while the remaining 25% consists of the same pattern but using elastic yarn (green in colour), to achieve an increased bending at the tip. The back panel is entirely crocheted with cotton yarn in *ts* -not extensible- pattern (red in colour).

Reducing both the both the length and width of the back panel further enhances the bending angle.

Both front and back are sewn together to form a finger-like actuator (or crocheted sleeve) as seen in Figure 26. When inserting a bladder inside the sleeve, the actuation path will result in the structure bending, since the front panel is more extensible than the back panel. This bending motion is one of the most common soft robotic systems (Figure 27).
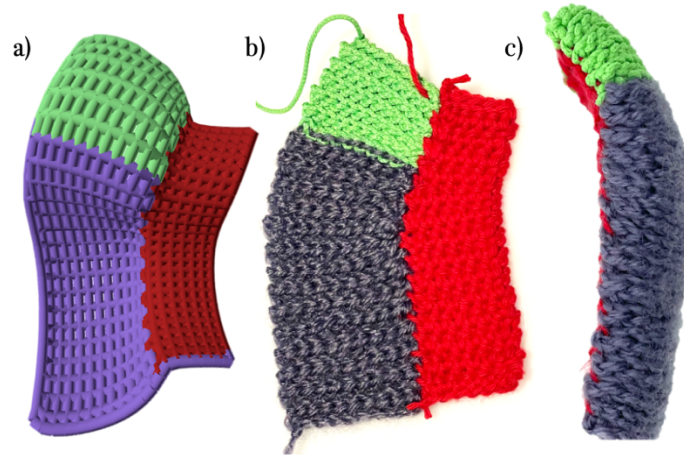
Figure 26. Fabrication of the crochet sleeve. (a) Simulation with CrochetPARADE. (b) Front and pack panel sewed on one side. (c) Panels sewed into a crocheted sleeve.
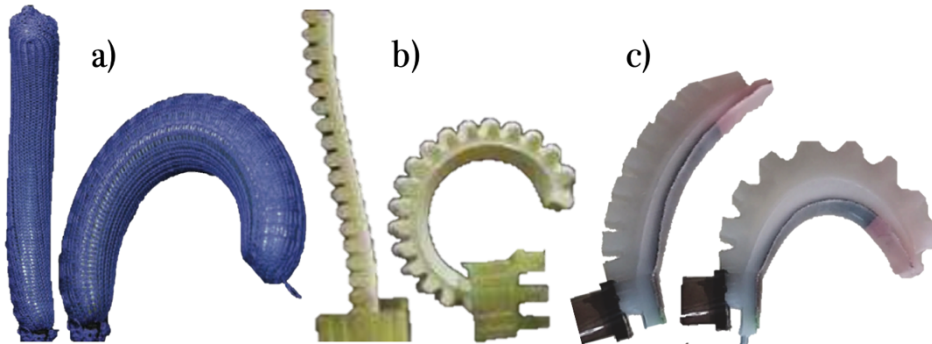
Figure 27. Several published pneumatic soft bending actuators of different manufacturing techniques: (a) knitted [30]. (b) 3D-printed with Ninja Flex [45]. (c) Silicone casted [43].

This design serves as the foundation for the fabrication of additional, similar structures. By altering the ratio of acrylic to elastic yarn in the front panel, the bending motion can be customised. Figure 28 illustrates this variation.
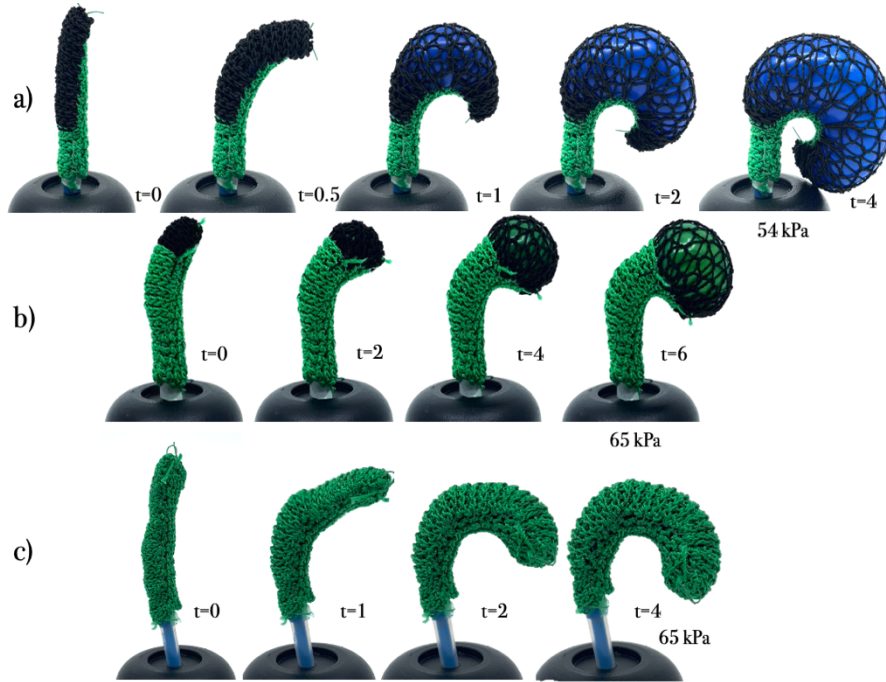
Figure 28. Bending motion of the actuators. Different curvatures are achieved by combining different yarns (acrylic in green, elastic in black). (a)30/70% acrylic to elastic. (b) 70/30% acrylic to elastic. (c)100% acrylic. Time stamps are measured in seconds.

A. Actuation Method

The crocheted sleeves are pneumatically actuated (i.e., airtight). Two distinct actuation methods were employed during the project.

-Balloon-actuation: Store-bought balloons served as the primary actuation mechanism. Two balloon models were used (Figure 29a) and cut to the appropriate length for each prototype. These balloons provided sufficient stability and force when inflated to suit the desired application. However, limitations arose due to their size and the substantial radial expansion required before significant length expansion occurred. This made them less suitable for smaller prototypes, such as the one shown in Figure 28 and the toroidal gripper in Figure 32.

-Silicone moulding-actuation: A 3D-printed mould was utilised to cast silicone through injection moulding, using *Ecoflex 00-30*. Figure 29b shows the setup, and Figure 29c demonstrates the crocheted sleeve actuated by the silicone balloon. This provided a more precise fit within the sleeve compared to the store-bought balloon, allowing also to cast a thinner base, thus, promoting lengthwise expansion. However, this technique was significantly more time-consuming and challenging. While silicone appears more promising for future prototypes, store-bought ballons were used due to time constraints throughout the project.
Both actuation methods were connected to a pneumatic plastic hose (*Festo PUN-H-4X0*) and sealed with thread-reinforcement and elastic tape.

B. Visualisation Tool. CrochetPARADE

CrochetPARADE (Crochet PAattern Renderer, Analyzer and DEebugger) is a platform designed to enable users to define stitches and patterns, generating a virtual model of crochet projects that can be rendered in 3D [44]. Once rendered, the platform allows users to debug the shape of the final project and make necessary adjustments. It also identifies areas with overly loose or tight stitches, helping to ensure uniform tension throughout. The platform allows users to pinpoint stitch connections and types by row number and position within each row. The software's grammar follows a structure similar to C++ syntax. It was developed by Svetlin Tassev.
A built-in library of common stitches is provided, each defined with the following notation:

*new_stitch=&stitch_name^top_nodes:bottom_nodes ~attachments::connections*

In this context:

-Top node refers to the upper part of a crochet stitch, where the hook is inserted. The bottom node is respectively the lower part of a stitch, the part that attaches with the stitch below. Loop insertion specifications can be defined here, such as [back] in the case of *ssbl*.

-Attachments define how the bottom and top node are connected, while connections specify the length between previous stitch and top node, and between top and bottom node. These values correspond to the length and height of each stitch, respectively. Detailed definitions of the stitches used in this project are provided in *Supplementary Information*.

3D visualisation canvas

The 3D model can be manipulated by adjusting the value of the *inflate* keyword. This parameter controls how distant stitches -not directly connected- interact, determining how much they push off each other to simulate the final structure. This process mimics pneumatic actuation. As the *inflate* value increases, the 3D model expands akin to inflating a ballon. Figure 30 presents a comparison between the simulated and fabricated actuators, showing different levels of actuation based on tunning the *inflate* parameter
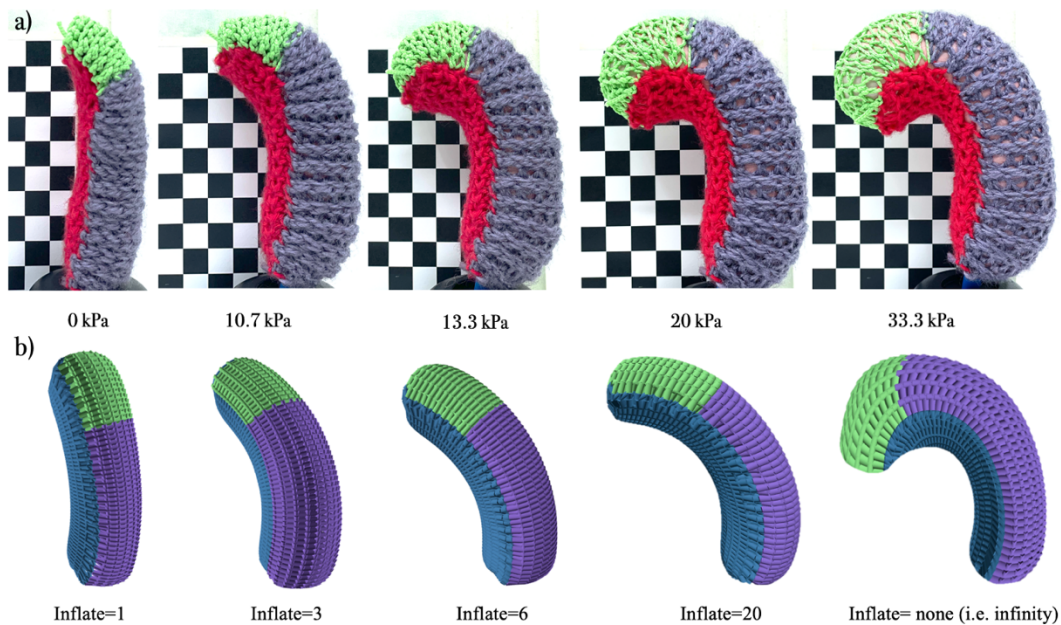
Figure 30. Bending of the actuator when comparing (a) the physical crocheted sleeve at different pressures (b) with the simulated one with CrochetPARADE for different Inflate parameters.

VI.   SOFT ROBOTIC APPLICATION DEMONSTRATIONS

In this section, we demonstrate the versatility of crocheted structures in the additive manufacturing of various soft robotic devices, including a three-finger-like gripper, a toroidal gripper, an inchworm-like robot, and an assistive glove.

All device design patterns were first created in CrochetPARADE to ensure the obtention of the desired final shape. The pattern instructions are included in *Supplementary Information*, and their 3D visualisation attached in each Figure*(a)*.

A.   *Three-Finger-Like Gripper*

Using the method described in *Section 5*. A three finger-like-gripper was fabricated. Two of the actuators were designed with a 70/30% *ssbl* acrylic-to-elastic yarn composition in the front panel, while the third one was entirely acrylic (Figure 31b). The back panel is fabricated with the stiff pattern -*ts*- and cotton yarn. This configuration allows two fingers to grasp, whilst the third one -having reduced bending- acts as a support for the grasped object. A 3D-printed structure was designed to couple the gripper with the end-effector of the UR3e robotic arm. The soft gripper can accommodate objects of varying shapes and weights, examples of which can be seen in Figure 31c.

To evaluate the gripping force, a pulling test was performed using the Instron machine. A 3D-printed cylindrical support was positioned at the base of the finger, which was then pressurised to enclose the cylinder. The cylinder was pulled upwards at a rate of 1mm/sec until the finger lost grip. To enhance adhesion and prevent slippage, two accessories were developed: a human-like nail and a silicone coating applied to the inner bottom of each finger. Figure 31d illustrates the experimental set up and Figure 31e the accessories.

Results are also deployed in Figure 31e, at a fixed pressure of 44kPa, the silicone-coated finger sustained a maximum gripping force of 10N. When comparing it with similar studies, results show forces up to 16N for a 3D-printed Ninja Flex finger [45], and 17N for a bellows-type foam bending actuator [46]. However, slippage still occurred within our test, which made a final assessment based on this experiment not conclusive.

Figure 31. (a) CrochetPARADE rendering of the gripper. (b) Final prototype with the 3D-printed UR3e support. (c) Gripper lifting various objects in shape and weight. (d) Experimental setup for the finger pulling test. (e) Results of the test at 44kPa.

B. Toroidal Gripper

A toroidal gripper was developed by combining an inextensible outer shell -cotton yarn, *ts* stitch-, with an acrylic yarn, *ssbl* stitch, as the extensible inner shell. Both shells were sewn together, forming a donut-like structure (Figure 32b). Upon pressurisation, the inner shell expands inwards to grasp objects, while the outer shell remains fixed in size due to the combination of material and pattern. This controlled, one-sided expansion is advantageous in applications where limited outer-deformation space is available. By controlling the amount of air inside the balloon, the expansion of the inner shell can be dictated, allowing conformity to the object being grasped, as seen in Figure 32c. The gripper is connected to the UR3.
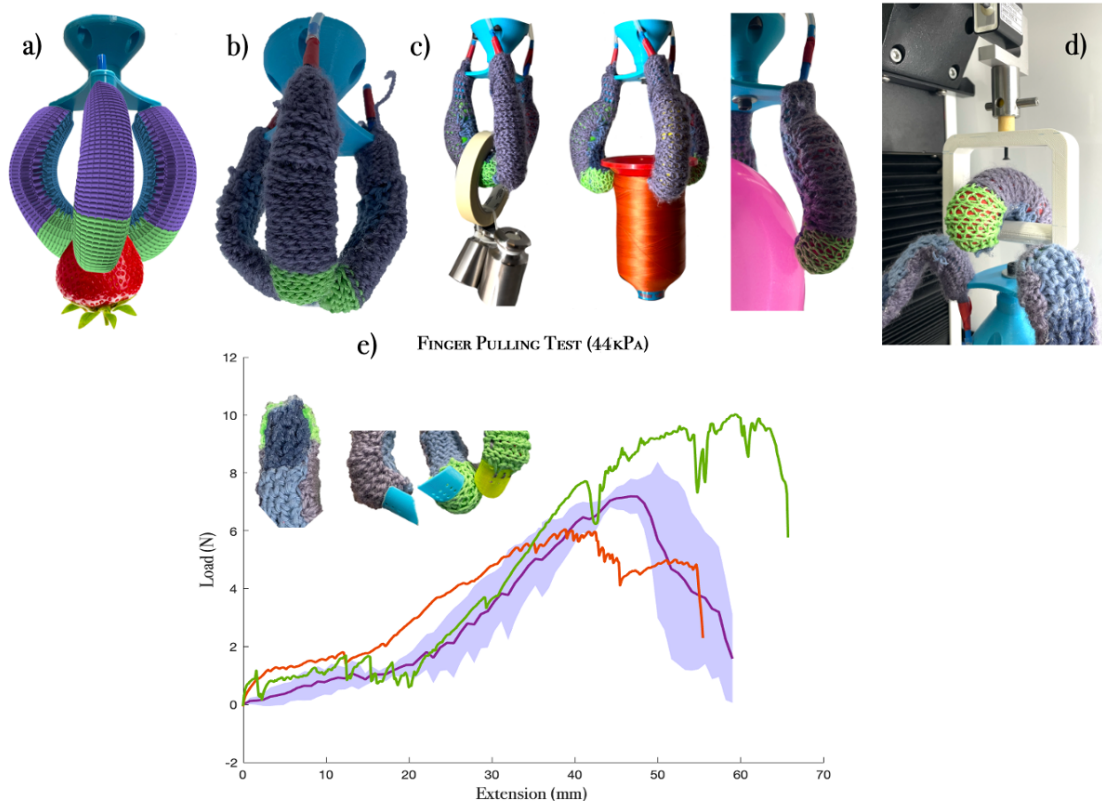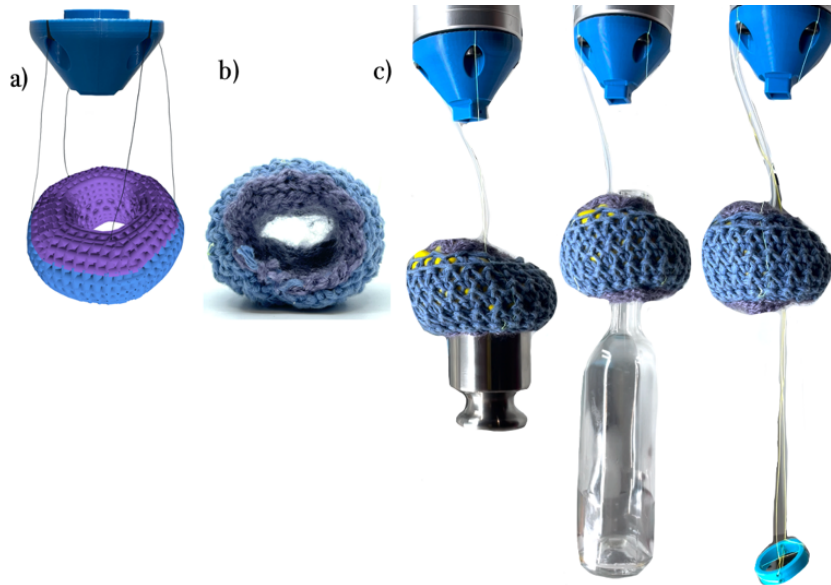
Figure 32. (a) CrochetPARADE rendering of the gripper. (b) Final prototype. (c) Gripper lifting various objects in shape and weight.

C. Peristaltic Spinchter Simulator

A variation of this toroidal shape involves crocheting a small tube that connects top and bottom sections. This shape is mathematically known as a Klein bottle [47] and can allow for liquids to flow inside the tube. When the inner shell is pressurised, flow is restricted, and ejection pressure increases. This movement can be mimicked with the mechanism of a heart valve and sphincters, (i.e., ring-shaped muscles that contract and relax, regulating the flow of substances through the body [48]). The anal sphincter comprises two muscles, an involuntary inner ring, and the outer ring which is under voluntary control. Peristaltic movements will allow the flow of stool from the rectum to the sphincter [49] as illustrated in Figure 33a. This whole process is simulated by fabricating three crocheted sphincters and, placing them around a knitted-silicone soft tube that simulates the rectum (Figure 33b).

To assess the performance of this device the following measurements were taken: the inner and outer actuator's shell expansion, the pressure that the actuators were able to withstand, and the pressure that the actuators built inside the soft tube. The setup is depicted in Figure 33c, and Figure 33d illustrates change of pressures when actuating the sphincter. The right plot shows that for an inflow pressure inside the tube of 40 kPa, when the valve is actuated (to 60 kPa), the pressure inside the tube builds up to 19 kPa. This pressure can be achieved in a gradual way, sustained for over 20 seconds, or rapidly released as the requirements dictate. The left plot deploys the same procedure but for an inner tube pressure inflow of 100 kPa, causing both the actuator's inner pressure and pressure inside the tube to increase. The inner expansion is 95%, while the outer one is 30%.

By actuating the three valves in a repetitive pattern, peristaltic movements can be simulated. Allowing liquids to get transferred from a chamber into a second one, as illustrated in Figure 34, the full motion can be found in *Supplementary Information*, Movie 2.
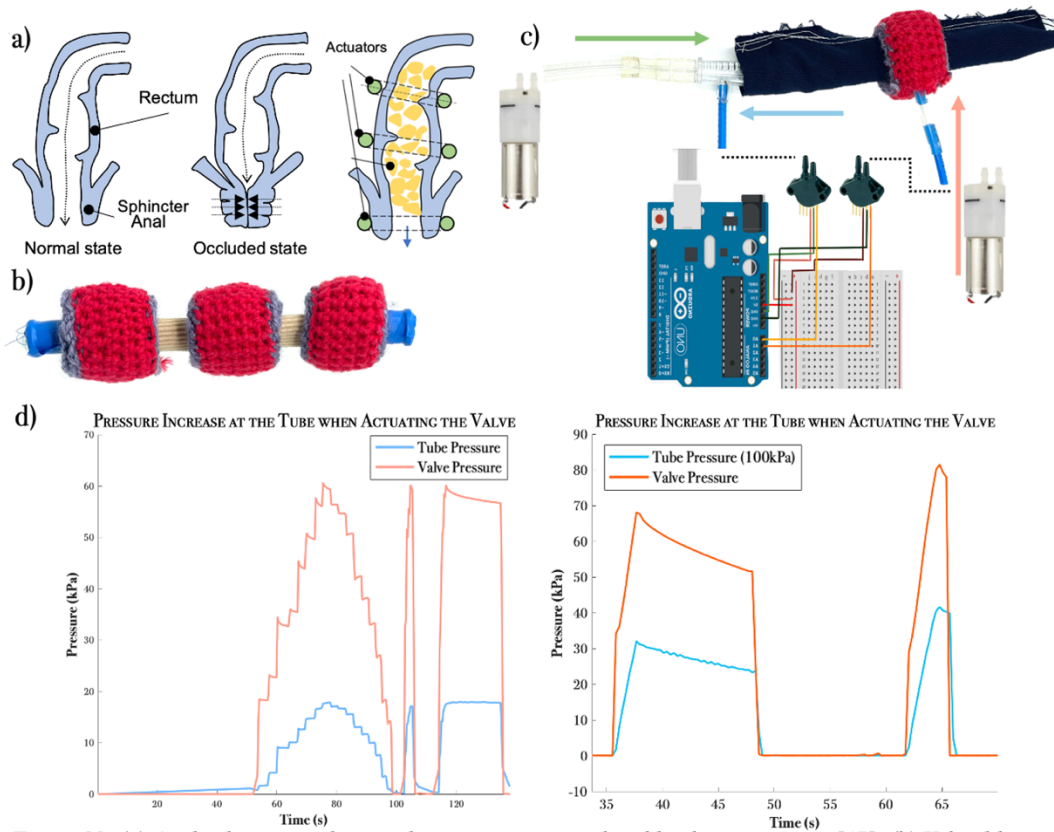
Figure 33. (a) Anal sphincter and peristaltic movements simulated by three actuators [47]. (b) Valve-like simulators around the knitted-silicone soft tube. (c) Measurements setup: 2 diaphragm pumps, 2 pressure sensors, Arduino Uno board, breadboard. (d) MATLAB plots, pressure increase inside the crocheted valve (in orange) vs pressure response inside the tube (in blue) to the valve being actuated. Tube inflow pressure 40 kPa and 100 kPa, respectively.

D. Inchworm-like Robot

Beyond grasping, more complex motions can be achieved by combining actuators with varying behaviours. An inchworm is an insect characterised by a long, flexible body, and two sets of short legs at each end [50]. By alternating between arching and stretching movements of the body and legs, it can crawl and climb on rough surfaces, as illustrated in Figure 35c. This locomotion pattern, known as Omega-shaped crawling, was replicated using three separate actuators: head and tail were fabricated with a *ssbl* front panel of 30/40/30% acrylic-elastic-acrylic composition, while the body is 5/90/5% acrylic-elastic-acrylic distribution in the x-direction (Figure 35b). The back panel is composed of *ts* pattern and cotton yarn, the head and tail actuators enable grasping, whilst the body achieves U-shaped bending.

The modular design allows the soft robot to move through confined spaces (Figure 35d), making it well-suited for applications such as search and rescue, exploration, and inspection in difficult-to-access areas that require flexible movements and minimal damage.
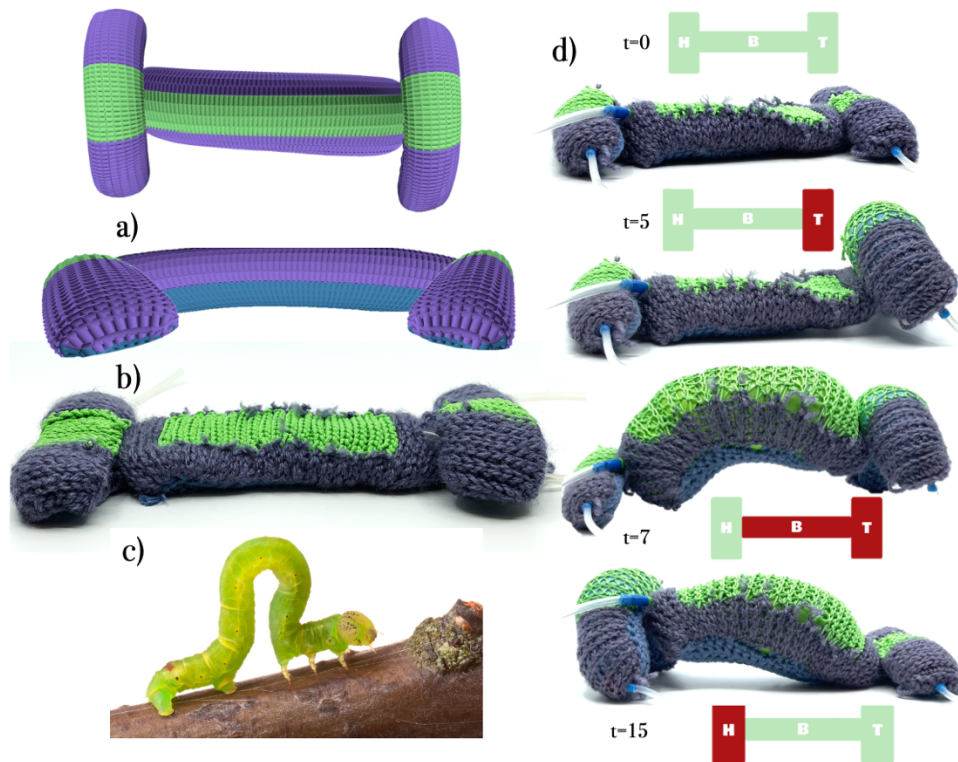
Figure 35. Inchworm-like Robot. (a) 3D rendering with CrochetPARADE. (b) Physical prototype. (c) Inchworm (3cm). (d) Inchworm-like floor locomotion, actuation time is deployed in seconds and next to it an illustration for which structure (head, body or tail) is being actuated (in red).

E. Gripping Assistive Glove

The fabrication of the assistive glove consisted of five actuators positioned at the dorsal side of each finger, as seen in Figure 36b. Each actuator is crocheted according to their paired finger, with a 70/30% acrylic-to-elastic yarn composition with *ssbl* pattern in the front panel to facilitate a forward bending motion, mimicking finger flexion, and enabling hand grasping. The back panel is entirely composed of cotton yarn with *ts* pattern. To further enhance this motion and provide additional stability, an elastic band connects each actuator to its respective finger. All five actuators are connected by a crocheted mesh across the hand. Figures 36b-d illustrate the movement. Each finger can be actuated individually, with a complete actuation cycle of approximately four seconds.

Figure 36e deploys a four second interval of an EMG measurement of the hand's primarily flexor muscle - *Flexor Digitorum Profundus*-. The first plot is recorded wearing the assistive glove, while for the second plot the subject is asked to perform grasping motions without the glove. The signal amplitude is reduced by half (from 10 to 5 mV) when the glove is being worn, these lower amplitudes indicate that the muscle requires less activation to perform the same task. Thus, the glove provides mechanical support, aiding finger flexion, which at its turn, reduces muscle fatigue.

This wearable device presents significant potential for individuals that have suffered an injury resulting in impaired hand function (e.g. stroke, neuromuscular conditions, comma), which hinders full grasping ability. Key factors contributing to such impairments include muscular weakness, reduced motor control, and involuntary muscle contractions [51]. The glove may be employed as an intermittent rehabilitation tool to support users in gradually regaining strength and coordination, or as a full-time assistive device to aid in daily activities that require gripping, squeezing, or holding objects for prolonged periods.

On a future perspective, the glove could be embedded with sensor technology providing real-time feedback on finger positions and, enabling users to gradually regain control through proprioceptive training. Nonetheless, the current crocheted device already offers notable advantages over traditional assistive devices, particularly in terms of lightweight construction, flexibility, and ease of use.

Unlike more rigid devices, this glove mimics the natural shape of the hand and provides dynamic support that facilitates movements rather that imposing static positions. Additionally, the yarn-based structure allows for a discreet, natural, and aesthetically pleasing appearance.
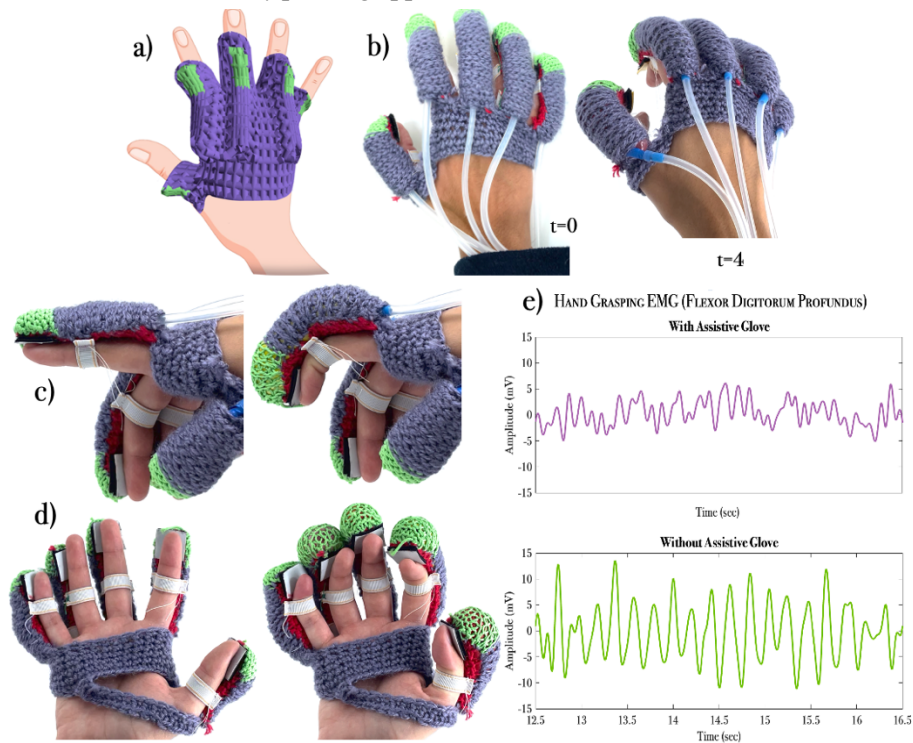
Figure 36. (a) CrochetPARADE rendering of the assistive glove. (b) Dorsal view of the hand. (c) Lateral view of the bending in the index finger. (d) Palmar view of the hand. Actuation time is in seconds. (e) 4 seconds of an EMG measurement of the Flexor Digitorum Profundus (located in the forearm) while grasping.

F. Additional Crocheted Biomedical Devices

More biomedical applications could arise from the experimental crocheted devices. For instance, by scaling down the size of the finger-like gripper, it could serve as a **soft endoscopic gripper**. When inserted into the human body, the textile's softness allows for a safe, effective manipulation of delicate tissues whilst minimising the risk of perforation, a key concern in current endoscopic procedures.

Furthermore, the crocheted sleeves themselves -without any pneumatic actuation- could serve therapeutic purposes as **compression garments**. By modifying the stitch pattern according to the degree of extensibility desired, garments can be tailored. Figure 37a shows a therapeutic glove designed with a stiff pattern -*ts*-. A garment ideal for users suffering from repetitive stress injuries (e.g., carpal tunnel syndrome) [52], while enabling natural motion for the hand –combination of non-stiff patterns- the thumb flexion, extension, abduction, and adduction motions are restraint, as well as reduced wrist movement (Figure 37b).
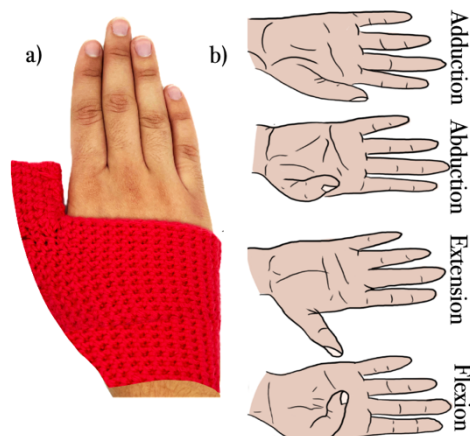
Figure 37. (a) Therapeutic Glove with ts stitch pattern. (b) Restricted thumb motions when wearing the glove.

Stents are used in medical procedures to restore blood flow in occluded arteries by applying pressure to the arterial wall until the narrowed sections open (Figure 38a) [53]. Achieving this requires high pressures to overcome the stiffness of the arterial wall. A compliant, crochet-based sleeve expandible under pressure was fabricated and tested as a stent-like device. The yarn and pattern configuration are the same as shown in Figure 28a.

Traditional aortic stents exert pressures in the range of 200-400 kPa to expand hardened or occluded walls, which exhibit significant resistance to expansion. Consequently, the stent's stiffness must be sufficient to maintain its expanded shape, typically ranging from 10 to 50 N/mm, depending on the degree of occlusion [54]. Using the aorta as a model, the key requirements include a wall thickness of 2-3mm, an inner radius of 10-15mm, and an average arterial expansion of 25%. Stiffness is calculated as follows

$$k_{stent} = \frac{P * A_{wall}}{\Delta r}, where\ A_{wall} = 2\pi rh$$

To achieve a value comparable to that of the aorta, two braided, expandable cable sleeves were used, one placed inside the other. Thickness was further increased by adding a knitted-silicone soft tube. The resulting wall thickness (h) was 3.5mm, with an inner radius of 15mm before expansion and 18mm after expansion. The pressure required to expand the cylindrical wall was of 85kPa, yielding a final stiffness of 9.35 N/mm. The setup for the measurements is shown in Figure 38b. The primary reason for the stiffness difference between conventional stents and our prototype is the significantly lower applied pressure. While the application has been proven feasible, and the prototype's behavior promising, future work will involve increasing the applied pressure to achieve a greater similarity to conventional stents.

Other applications -opening of the airways for inspection- may involve body areas that do not require as high pressures (i.e., structural rigidity). For instance, using only the silicone-knitted tube, radial elongations of 80-90% are achieved with applied pressures of 53-56 kPa (Figure 38c).
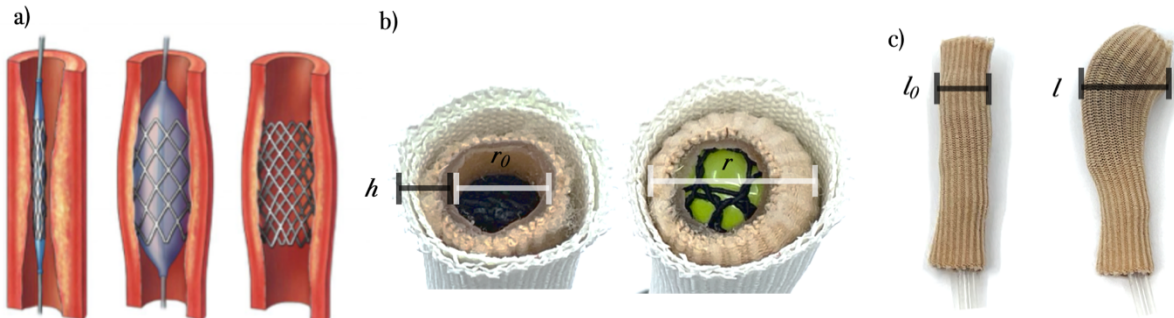
Figure 34. Stent-like device. (a) Conventional ballooning stent [52]. (b) Crocheted sleeve inside two white braided cable sleeves and a soft silicone knitted tube, before and after expansion (top to bottom). (c) Expansion of the crocheted sleeve inside the soft silicone knitted tube.

Table 9 presents some key metrics important to variable-stiffness prototype fabrication[55].

TABLE VII.   STIFFNESS KEY METRICS OF THE PROTOTYPES

METRICS	Finger Gripper	Toroidal Gripper	Inchworm Robot	Assistive Glove
Hard-to-Soft Cycle (sec)	9	4	17	4
Maximum Weight (g)	170	150	NA	N/A
Movement (mm)	N/A	N/A	9	50
Radial ΔL (%)	N/A	30	N/A	N/A
Maximum Pressure (kPa)	44	35	25	48

VII. LIMITATIONS AND FUTURE WORK

The limitations of the study can be categorised in four key areas: mechanical modelling, tensile testing, visualization software, and prototype development.

A. Testile Testing Experiments

- Despite efforts to maintain consistent initial tension at the Instron clamps, small variations may have occurred. This could be mitigated in future work by incorporating a camera system for real-time calibration of the machine.

- The Instron only allows for uniaxial tensile experiments. Expanding this to include biaxial testing would provide a more comprehensive understanding of the mechanical properties. This becomes relevant for stiffness-control of actuators, which extend both in the x- and y-directions.

B. Mechanical Modelling

- The current model predicts only the maximum stiffness at a given load. Future work should involve training a MATLAB model to predict the full stiffness curve, enhancing the understanding of stiffness variations throughout the actuation cycle.

- The model has been validated only for 30 and 15N loads. However, since stiffness plateaus above 10 and 15N, validation for lower loads would be beneficial to extend the model's applicability.

- The model underestimates stiffness values for ts stitch pattern at high loads. This issue could be addressed by training a more advanced curve-prediction algorithm.

C. Visualisation Software -CrochetPARADE-

- CrochetPARADE does not account for the intrinsic material properties of the yarn, limiting its ability to accurately render actuated models –only stitch patterns account for the extensibilities' degree-.

- Adjusting the 'Inflate' parameter significantly delays the rendering process, which introduces accuracy errors in the 3D model's final output.

D. Final Applications

The actuation methods have limitations. Store-bought ballons, whilst quick to implement, tend to exhibit excessive radial expansion, resulting in inconsistent deformations. Silicone moulding, though more precise, is time-consuming, limiting its practicality for rapid prototyping. Future work should explore alternative actuation methods that address both time-efficiency and precision.

E. Future Work

- Additional application-oriented testing on the fabricated actuators is required to fully characterise their capabilities.

- Sourcing custom yarns with tailored mechanical properties (e.g., biocompatible, conductive, or smart yarns) could enhance control over the stiffness and overall actuator's performance.

- The later step, combined with embedded sensors could provide real-time feedback. This would improve not only the overall control over the actuation itself, but also open new possibilities for biomedical assistive devices.

VIII. CONCLUSION

This study presents an approach for controlling the stiffness and actuation of crocheted soft robots by manipulating stitch patterns and yarn materials.

In soft robotics, particularly for applications in endoscopic or surgical operations, extraordinary flexibility is essential to perform simple tasks while maintaining the capability to exert high and precise forces. For instance, 2 to 6 N are required for a suturing task, which underscores the importance of stiffness tunability in such robotic systems. To address these requirements, this work models the mechanical behaviour of crochet swatches using a topology-based framework, treating each stitch as a spring with unique stiffness characteristics. The results successfully capture the relationship between stitch patterns, material properties, and stiffness under tensile loads, enabling accurate predictions of stiffness behaviour. For instance, cotton swatches exhibit stiffness values ranging from 2-5 N/mm based solely on stitch pattern variations, with an associated extension difference of 55mm. In contrast, elastic swatches maintain a stiffness of 2N/mm across patterns but exhibit an extension difference of 100mm. This tuneable range in stiffness and extensibility, emphasises the potential of crochet to provide customisable mechanical properties within a single material system.

The tuning of crocheted mechanical properties allows for several motions within the realm of soft robotic systems, with a particular emphasis on the biomedical field. Prototypes include a soft gripper, crocheted sleeves with programmable expansion, a toroidal gripper able to mimic valves, and an assistive glove for enhancing grasping capabilities. While the mechanical model and fabrication methods demonstrate novelty and promise, several limitations remain. Key future developments include improving the mechanical model, enhancing the rendering of 3D crocheted structures, and developing a machine capable of automatising the crochet manufacturing process. These advancements will pave the way for integrating 3D crocheted structures into the research domains of technical textiles and soft robotics. As such, this study contributes its novelty in this field, showcasing the unique mechanical adaptability of crochet as a manufacturing method capable of fabricating bio-inspired robotic designs.

iii. REFERENCES

[1] T. Ashuri, A. Armani, R. Jalilzadeh Hamidi, T. Reasnor, S. Ahmadi, and K. Iqbal, "Biomedical soft robots: current status and perspective," Biomedical Engineering Letters, vol. 10, no. 3, pp. 369–385, Aug. 2020, doi: 10.1007/s13534-020-00157-6.

[2] D. Trivedi, C. D. Rahn, W. M. Kier, and I. D. Walker, "Soft robotics: Biological inspiration, state of the art, and future research," *Applied Bionics and Biomechanics*, vol. 5, no. 3, pp. 99–117, 2008, doi: 10.1080/11762320802557865.

[3] Webster RJ, Jones BA. Design and kinematic modeling of con- stant curvature continuum robots: a review. Int J Robot Res. 2010;29(13):1661–83. https://doi.org/10.1177/0278364910368147.

[4] A. D. Marchese, C. D. Onal, and D. Rus, "Autonomous Soft Robotic Fish Capable of Escape Maneuvers Using Fluidic Elastomer Actuators," *Soft Robotics*, vol. 1, no. 1, pp. 75–87, Mar. 2014, doi: 10.1089/SORO.2013.0009.

[5] X. Lu, W. Xu, and X. Li, "A Soft Robotic Tongue-Mechatronic Design and Surface Reconstruction," *IEEE/ASME Transactions on Mechatronics*, vol. 22, no. 5, pp. 2102–2110, Oct. 2017, doi: 10.1109/TMECH.2017.2748606.

[6] M. Cianchetti, C. Laschi, A. Menciassi, and P. Dario, "Biomedical applications of soft robotics," *Nature Reviews Materials*, vol. 3, no. 6, pp. 143–153, Jun. 2018, doi: 10.1038/S41578-018-0022-Y.

[7] Higuchi T, Suzumori K, Tadokoro S, editors. Next-generation actuators leading breakthroughs. New York: Springer; 2010.

[8] D. Jayatilake and K. Suzuki, "A soft actuator based expressive mask for facial paralyzed patients," *2008 IEEE/RSJ International Conference on Intelligent Robots and Systems, IROS*, pp. 4048–4053, 2008, doi: 10.1109/IROS.2008.4651177.

[9] B. B. Kang, H. Lee, H. In, U. Jeong, J. Chung, and K. J. Cho, "Development of a polymer-based tendon-driven wearable robotic hand," *Proceedings - IEEE International Conference on Robotics and Automation*, vol. 2016-June, pp. 3750–3755, Jun. 2016, doi: 10.1109/ICRA.2016.7487562.

[10] P. Polygerinos, Z. Wang, K. C. Galloway, R. J. Wood, and C. J. Walsh, "Soft robotic glove for combined assistance and at-home rehabilitation," *Robotics and Autonomous Systems*, vol. 73, pp. 135–143, Nov. 2015, doi: 10.1016/J.ROBOT.2014.08.014.

[11] E. T. Roche *et al.*, "Soft robotic sleeve supports heart function," *Science translational medicine*, vol. 9, no. 373, Jan. 2017, doi: 10.1126/SCITRANSLMED.AAF3925.

[12] Weber J, Robaina S. (2010). U.S. Patent No. 7,767,219. Washington, DC: U.S. Patent and Trademark Office.

[13] "Medical balloon incorporating electroactive polymer and methods of making and using the same - Patent US-7777399-B2 - PubChem." Accessed: Sep. 26, 2024. [Online]. Available: https://pubchem.ncbi.nlm.nih.gov/patent/US-7777399-B2

[14] A. Diodato *et al.*, "Soft Robotic Manipulator for Improving Dexterity in Minimally Invasive Surgery," *Surgical Innovation*, vol. 25, no. 1, pp. 69–76, Feb. 2018, doi: 10.1177/1553350617745953.

[15] Y. Luo *et al.*, "Digital Fabrication of Pneumatic Actuators with Integrated Sensing by Machine Knitting," *Conference on Human Factors in Computing Systems - Proceedings*, Apr. 2022, doi: 10.1145/3491102.3517577.

[16] J. Walker *et al.*, "Soft Robotics: A Review of Recent Developments of Pneumatic Soft Actuators," *Actuators*, vol. 2020, p. 3, 2015, doi: 10.3390/act9010003.

[17] X. Jing, S. Chen, C. Zhang, and F. Xie, "Machines Increasing Bending Performance of Soft Actuator by Silicon Rubbers of Multiple Hardness," 2022, doi: 10.3390/machines10040272.

[18] L. Wu, F. Zhao, J. Xie, X. Wu, Q. Jiang, and J. H. Lin, "The deformation behaviors and mechanism of weft knitted fabric based on micro-scale virtual fiber model," *International Journal of Mechanical Sciences*, vol. 187, p. 105929, Dec. 2020, doi: 10.1016/J.IJMECSCI.2020.105929.

[19] T. Ashuri, A. Armani, R. Jalilzadeh Hamidi, T. Reasnor, S. Ahmadi, and K. Iqbal, "Biomedical soft robots: current status and perspective," *Biomedical Engineering Letters*, vol. 10, no. 3, p. 369, Aug. 2020, doi: 10.1007/S13534-020-00157-6.

[20] "The History of Crochet | Darn Good Yarn." Accessed: Nov. 06, 2024. [Online]. Available: https://www.darngoodyarn.com/blogs/darn-good-blog/crafting-in-history-the-history-of-crochet?srsltid=AfmBOopj_rYytu-ZPMRbHwTRIEKa3uYIZYp4vig6wVpJJsP1M7VuHiRd

[21] "Knitting vs. Crochet - What's the difference? | Gathered." Accessed: Nov. 06, 2024. [Online]. Available: https://www.gathered.how/knitting-and-crochet/crochet/crochet-vs-knitting-difference

[22] K. Seitz, J. Lincke, P. Rein, and R. Hirschfeld, "Language and tool support for 3D crochet patterns : virtual crochet with a graph structure," no. 137, 2021, doi: 10.25932/PUBLISHUP-49253.

[23] D. W. Henderson and D. Taimina, "Crocheting thc Hyperbolic Planc," 2001.

[24] F. M. Schipper, "A Mathematical Study of Crochet".

[25] C. Jiang, K. Wang, Y. Liu, C. Zhang, and B. Wang, "Textile-based sandwich scaffold using wet electrospun yarns for skin tissue engineering," *Journal of the Mechanical Behavior of Biomedical Materials*, vol. 119, p. 104499, Jul. 2021, doi: 10.1016/J.JMBBM.2021.104499.

[26] M. Bobin, H. Amroun, S. Coquillart, F. Bimbard, and M. Ammi, "SVM based approach for the assessment of elbow flexion with smart textile sensor," *2017 IEEE International Conference on Systems, Man, and Cybernetics, SMC 2017*, vol. 2017-January, pp. 2129–2134, Nov. 2017, doi: 10.1109/SMC.2017.8122934.

[27] Z. Xu, Y. Matsuoka, and A. D. Deshpande, "Crocheted artificial tendons and ligaments for the anatomically correct testbed (ACT) hand," *2015 IEEE International Conference on Robotics and Biomimetics, IEEE-ROBIO 2015*, pp. 2449–2453, 2015, doi: 10.1109/ROBIO.2015.7419706.

[28] G. Perry, J. L. G. del Castillo Y Lopez, and N. Melenbrink, "Croche-Matic: a robot for crocheting 3D cylindrical geometry," *Proceedings - IEEE International Conference on Robotics and Automation*, vol. 2023-May, pp. 7440–7446, 2023, doi: 10.1109/ICRA48891.2023.10160345.

[29] C. Karp, "Defining Crochet," *Textile History*, vol. 49, no. 2, pp. 208–223, Jul. 2018, doi: 10.1080/00404969.2018.1491689.

[30] V. Sanchez *et al.*, "3D Knitting for Pneumatic Soft Robotics," *Advanced Functional Materials*, vol. 33, no. 26, Jun. 2023, doi: 10.1002/ADFM.202212541.

[31] K. Singal, M. S. Dimitriyev, S. E. Gonzalez, A. P. Cachine, S. Quinn, and E. A. Matsumoto, "Programming mechanics in knitted materials, stitch by stitch," *Nature Communications 2024 15:1*, vol. 15, no. 1, pp. 1–9, Mar. 2024, doi: 10.1038/s41467-024-46498-z.

[32] Y. Luo *et al.*, "Digital Fabrication of Pneumatic Actuators with Integrated Sensing by Machine Knitting," *Conference on Human Factors in Computing Systems - Proceedings*, Apr. 2022, doi: 10.1145/3491102.3517577.

[33] S. Poincloux, M. Adda-Bedia, and F. Lechenault, "Geometry and Elasticity of a Knitted Fabric," *Physical Review X*, vol. 8, no. 2, p. 021075, Jun. 2018, doi: 10.1103/PHYSREVX.8.021075/FIGURES/10/MEDIUM.

[34] J. L. Storck, D. Gerber, L. Steenbock, and Y. Kyosev, "Topology based modelling of crochet structures," *Journal of Industrial Textiles*, vol. 52, Jul. 2022, doi: 10.1177/15280837221139250.

[35] J. L. Storck, L. Steenbock, M. Dotter, H. Funke, and A. Ehrmann, "Principle capabilities of crocheted fabrics for composite materials," *Journal of Engineered Fibers and Fabrics*, vol. 18, Jan. 2023, doi: 10.1177/15589250231203381.

[36] "Geometric and Mechanical Modelling of Textiles." Accessed: Nov. 06, 2024. [Online]. Available: https://www.researchgate.net/publication/37245662_Geometric_and_Mechanical_Modelling_of_Textiles

[37] "Out of Production 3300 Series Universal Testing Systems | Instron." Accessed: Nov. 06, 2024. [Online]. Available: https://www.instron.com/en/products/testing-systems/universal-testing-systems/low-force-universal-testing-systems/3300-series

[38] "MSE 527L-Testing of Materials in Tension". Accesed: Nov. 06, 2024. [Online]. Available: https://www.csun.edu/~bavarian/Courses/MSE%20527/Tension_test_MSE_527L.pdf

[39] F. Baumgart, "Stiffness – an unknown world of mechanical science?," *Injury*, vol. 31, no. SUPPL.2, pp. 14–84, May 2000, doi: 10.1016/S0020-1383(00)80040-6.

[40] "Stress/Strain Evaluation of Fibers Using TMA", Accessed: Jun. 03, 2024. [Online]. Available: https://www.tainstruments.com/pdf/literature/TA414.pdf

[41] "Modulus of Elasticity | Instron." Accessed: May 06, 2024. [Online]. Available: https://www.instron.com/en/resources/glossary/modulus-of-elasticity

[42] B. Gommers, I. Verpoest, and P. Houtte, "Analysis of knitted fabric reinforced composites: Part II. Stiffness and strength," *Composites Part A: Applied Science and Manufacturing*, vol. 29, no. 12, pp. 1589–1601, Dec. 1998, doi: 10.1016/S1359-835X(98)00096-7.

[43] N. Gariya, P. Kumar, and T. Singh, "Experimental study on a bending type soft pneumatic actuator for minimizing the ballooning using chamber-reinforcement," *Heliyon*, vol. 9, no. 4, p. e14898, Apr. 2023, doi: 10.1016/J.HELIYON.2023.E14898.

[44] "CrochetPARADE." Accessed: Nov. 06, 2024. [Online]. Available: https://www.crochetparade.org/

[45] H. K. Yap, H. Y. Ng, and C. H. Yeow, "High-Force Soft Printable Pneumatics for Soft Robotic Applications," *Soft Robotics*, vol. 3, no. 3, pp. 144–158, Sep. 2016, doi: 10.1089/SORO.2016.0030.

[46] K. C. Galloway *et al.*, "Soft Robotic Grippers for Biological Sampling on Deep Reefs," *Soft Robotics*, vol. 3, no. 1, pp. 23–33, Mar. 2016, doi: 10.1089/SORO.2015.0019.

[47] "Botella de Klein - Wikipedia, la enciclopedia libre." Accessed: Nov. 02, 2024. [Online]. Available: https://es.wikipedia.org/wiki/Botella_de_Klein

[48] "Definition of sphincter - NCI Dictionary of Cancer Terms - NCI." Accessed: Nov. 02, 2024. [Online]. Available: https://www.cancer.gov/publications/dictionaries/cancer-terms/def/sphincter

[49] Z. Mao, S. Suzuki, A. Wiranata, Y. Zheng, and S. Miyagawa, "Bio-inspired circular soft actuators for simulating defecation process of human rectum," *Journal of artificial organs : the official journal of the Japanese Society for Artificial Organs*, 2024, doi: 10.1007/S10047-024-01477-5.

[50] "Measuring worm | Inchworm, Caterpillar, Larva | Britannica." Accessed: Nov. 02, 2024. [Online]. Available: https://www.britannica.com/animal/measuring-worm

[51] P. Polygerinos *et al.*, "Towards a soft pneumatic glove for hand rehabilitation," *IEEE International Conference on Intelligent Robots and Systems*, pp. 1512–1517, 2013, doi: 10.1109/IROS.2013.6696549.

[52] "Carpal tunnel syndrome - NHS." Accessed: Nov. 02, 2024. [Online]. Available: https://www.nhs.uk/conditions/carpal-tunnel-syndrome/

[53] "Endoprótesis (stents) - Colocación de una endoprótesis | NHLBI, NIH." Accessed: Oct. 29, 2024. [Online]. Available: https://www.nhlbi.nih.gov/es/salud/endoprotesis/durante

[54] C. Lally, F. Dolan, and P. J. Prendergast, "Cardiovascular stent design and vessel stresses: a finite element analysis," *Journal of Biomechanics*, vol. 38, no. 8, pp. 1574–1581, Aug. 2005, doi: 10.1016/J.JBIOMECH.2004.07.022.

[55] Z. Yang, X. Li, R. Chen, D. Shang, J. Xu, and H. Yang, "Dynamic performance analysis of the variable stiffness actuator considering gap and friction characteristics based on two-inertia-system," *Mechanism and Machine Theory*, vol. 168, p. 104584, Feb. 2022, doi: 10.1016/J.MECHMACHTHEORY.2021.104584.

iv. SUPPLEMENTARY INFORMATION

1. Model prediction tables

TABLE I.   KPREDICTED VS KMATLAB TO ASSES THE ACCURACY OF THE MODEL

Predicted Stiffness (N/mm)	Yarn and Pattern					
	Cotton		Acrylic		Polyamide	
	ssbl	ts	ssbl	ts	ssbl	ts
Full swatch	2.12	4.29	1.78	2.26	0.85	1.13
7 Rows	3.54	6.01	2.96	3.08	1.41	1.54
5 Rows	5.31	10.01	3.81	4.24	1.81	2.12
3 Rows	7.96	15.02	6.67	8.48	3.18	4.23

MATLAB Stiffness (N/mm)	Yarn and Pattern					
	Cotton		Acrylic		Polyamide	
	ssbl	ts	ssbl	ts	ssbl	ts
Full swatch	2.39	4.42	2.37	2.68	1.07	1.33
7 Rows	3.09	6.31	3.51	3.39	1.5	1.64
5 Rows	4.39	10.2	3.64	4.57	1.71	2.19
3 Rows	6.15	13.98	4.49	6.53	2.07	2.82

TABLE II.   KPREDICTED VS KMATLAB TO VALIDATE THE MODEL.

Predicted Stiffness (N/mm)	Yarn and Pattern					
	Cotton		Acrylic		Polyamide	
	ssbl	ts	ssbl	ts	ssbl	ts
1 row	17.3	28.3	-	-	-	-
4 rows	-	-	4.45	5.56	-	-
6 rows	-	-	-	-	1.41	1.88
Validation Swatches	2.45	4.62	2.05	2.61	0.98	1.3
Validation Swatches 15N	1.23	2.31	1.03	1.3	0.49	0.65

MATLAB Stiffness (N/mm)	Yarn and Pattern					
	Cotton		Acrylic		Polyamide	
	ssbl	ts	ssbl	ts	ssbl	ts
1 row	15.2	35.81	-	-	-	-
4 rows	-	-	4.48	5.91	-	-
6 rows	-	-	-	-	0.83	1.12
Validation Swatches	1.47	2.8	1.88	2.04	0.9	0.86
Validation Swatches 15N	0.78	1.75	0.76	0.98	0.36	0.42

2. CrochetPARADE basic stitches definition:

```
Double_crochet= &dc^A(dc):B~A-B::!-1-A;B-2-A

Half_double_crochet= &hdc^A(hdc):B~A-B::!-1-A;B-1.5-A

Single_crochet= &sc^A(sc):B~A-B::!-1-A;B-1-A

Slip_stitch_back_loop= &ssbl^A(ssbl):B[back]~A-B::!-1-A;B-0.4-A

Thermal_stitch= &ts^A(sc):B1[back];B2[back]~A-B::!-1-A;B-1-A
```

3. CrochetPARADE 3D pattern instructions:

Individual Gripper Actuators

```
BACKGROUND: White
COLOR: Steel Blue, 8ch,turn
sk,(hdc2inc,5hdc,hdc3inc).R,turn
COLOR: Light Green,(hdc@[0,1],4hdc,hdc2inc).R,ss@[0,-1]
ch,(hdc2inc,7hdc,hdc2inc,COLOR: Steel Blue,2hdc2inc,7hdc,hdc2inc)@R,hdc@[-1,-1],ss@[%,0]
ch,COLOR: Light Green,16ssbl,COLOR: Steel Blue,9ss,ss@[%,0]
[ch,sk,COLOR: Light Green,16ssbl,COLOR: Steel Blue,9ss,ss@[ch:%,0]
]*13
[ch,sk,COLOR: Medium Purple,16ssbl,COLOR: Steel Blue,9ss,ss@[ch:%,0]
]*37
ch,sk,COLOR: Medium Purple,6ss,ss2tog,6ss,ss2tog,COLOR: Steel Blue,7ss,ss2tog,ss@[ch:%,0]
ch,sk,COLOR: Medium Purple,5ss,ss2tog,5ss,ss2tog,COLOR: Steel Blue,6ss,ss2tog,ss@[ch:%,0]
ch,sk,COLOR: Medium Purple,4ss,ss2tog,4ss,ss2tog,COLOR: Steel Blue,5ss,ss2tog,ss@[ch:%,0]
ch,sk,COLOR: Medium Purple,3ss,ss2tog,3ss,ss2tog,COLOR: Steel Blue,5ss,ss2tog,ss@[ch:%,0]
```

Toroidal Gripper

```
BACKGROUND: White
COLOR: Medium Purple,30ch,ss@[0,29]
30sc
30sc
30sc
[4sc,sc2inc]*6
[5ss,sc2inc]*6
[6sc,sc2inc]*6
[7sc,sc2inc]*6
COLOR: Cornflower Blue,[8sc,sc2inc]*6
[9sc,sc2inc]*6
66sc
66sc
66sc
[9sc,sc2tog]*6
COLOR: Medium Purple,[8sc,sc2tog]*6
[7sc,sc2tog]*6
[6sc,sc2tog]*6
[5sc,sc2tog]*6
[4sc,sc2tog]*6
30sc
30sc
30sc
30sc
sc@[0,0],sc@[22,1],sc@[0,2],sc@[22,3],sc@[0,4],sc@[22,5],sc@[0,6],sc@[22,7],sc@[0,8],sc@[22,9],sc
@[0,10],sc@[22,11],sc@[0,12],sc@[22,13],sc@[0,14],sc@[22,15],sc@[0,16],sc@[22,17],sc@[0,18],sc@[2
2,19],sc@[0,20],sc@[22,21],sc@[0,22],sc@[22,23],sc@[0,24],sc@[22,25],sc@[0,26],sc@[22,27],sc@[0,2
8],sc@[22,29]
```

Assistive Gripper:

```
BACKGROUND: White
COLOR:Medium Purple,32ch,ss@[%,0]
COLOR: Medium Purple,ch,sk,[31sc,ss@[%,0]
]*5
ch,sk,31hdc.R,ss@[%,0]
ch,(2hdc2inc,11hdc,4hdc2inc,11hdc,2hdc2inc)@R,hdc@[-1,-1],ss@[%,0]
ch,sk,34hdc,4sk
3ch,3sk,35hdc,ss@[%,0]
ch,sk,[38hdc,ss@[%,0]
]*6
6hdc,ss@[%-1,32],turn
[13hdc,ss@[%,0]
]*3
start_at@[16,5],ch,hdc@[15,6],hdc@[15,7],hdc@[15,8],hdc@[15,9],hdc@[15,10],ss@[15,27],turn
hdc@[15,28],hdc@[15,29],hdc@[15,30],hdc@[15,31],hdc@[15,32],ss@[20,0]
ch,hdc@[20,1],hdc@[20,2],hdc@[20,3],hdc@[20,4],hdc@[20,5],hdc@[20,6],hdc@[20,7],hdc@[21,0],hdc@[2
1,1],hdc@[21,2],hdc@[21,3],hdc@[21,4],hdc@[21,5],ss@[%,0]
[12hdc,ss@[%,0]
]*2
start_at@[20,7],ch,hdc@[15,27],hdc@[15,26],hdc@[15,25],hdc@[15,24],hdc@[15,23],ss@[15,15],ch,hdc@
[15,14],hdc@[15,13],hdc@[15,12],hdc@[15,11],ss@[20,7],ss@[%,0]
[11hdc,ss@[%,0]
]*3
start_at@[25,6],ch,hdc@[15,23],hdc@[15,22],hdc@[15,21],hdc@[15,20],hdc@[15,19],hdc@[15,18],hdc@[1
5,17],hdc@[15,16],ss@[25,7],ss@[%,0]
[10hdc,ss@[%,0]
]*2
start_at@[9,0],ch,hdc@[9,2],hdc@[8,3],hdc@[8,0],hdc@[7,40],hdc@[7,39],hdc@[7,38],hdc@[7,37],hdc@[
7,36],hdc@[7,35],ss@[%,0]
[13hdc,ss@[%,0]
]*2

COLOR: Medium Purple,start_a_new_chain,9ch,turn
COLOR: Light Green,ch,sk,3ss,COLOR: Medium Purple,6ss,turn
COLOR: Medium Purple,ch,sk,6ss,COLOR: Light Green,3ss,turn
COLOR: Light Green,ch,sk,3ss,COLOR: Medium Purple,6ss,turn
COLOR: Medium Purple,ch,sk,6ss,COLOR: Light Green,3ss,turn
COLOR: Medium
Purple,start_at@[39,9],sc@[18,5],sc@[39,8],sc@[17,5],sc@[39,7],sc@[16,2],sc@[39,6],sc@[15,2],sc@[
39,5],sc@[14,2],sc@[39,4],sc@[13,2],sc@[39,3],sc@[12,2],sc@[39,2],sc@[11,2],sc@[39,1],sc@[10,2],s
c@[39,0]
start_at@[36,0],sc@[18,3],sc@[38,0],sc@[18,4]
```

```
start_at@[35,9],sc@[18,1],sc@[35,8],sc@[17,1],sc@[35,7],sc@[16,5],sc@[35,6],sc@[15,5],sc@[35,5],s
c@[14,5],sc@[35,4],sc@[13,5],sc@[35,3],sc@[12,5],sc@[35,2],sc@[11,5],sc@[35,1],sc@[10,5],sc@[35,0
]
start_at@[39,0],sc@[10,3],sc@[36,9],sc@[10,4]

COLOR: Medium Purple,start_a_new_chain,9ch,turn
COLOR: Light Green,ch,sk,3ss,COLOR: Medium Purple,6ss,turn
COLOR: Medium Purple,ch,sk,6ss,COLOR: Light Green,3ss,turn
COLOR: Light Green,ch,sk,3ss,COLOR: Medium Purple,6ss,turn
COLOR: Medium Purple,ch,sk,6ss,COLOR: Light Green,3ss,turn
COLOR: Medium
Purple,start_at@[48,9],sc@[23,5],sc@[48,8],sc@[22,5],sc@[48,7],sc@[20,5],sc@[48,6],sc@[15,9],sc@[
48,5],sc@[14,9],sc@[48,4],sc@[13,9],sc@[48,3],sc@[12,9],sc@[48,2],sc@[11,9],sc@[48,1],sc@[10,9],s
c@[48,0]
start_at@[44,9],sc@[23,2],sc@[44,8],sc@[22,2],sc@[44,7],sc@[20,2],sc@[44,6],sc@[15,6],sc@[44,5],s
c@[14,6],sc@[44,4],sc@[13,6],sc@[44,3],sc@[12,6],sc@[44,2],sc@[11,6],sc@[44,1],sc@[10,6],sc@[44,0
]
start_at@[45,9],ss@[10,7],ss@[48,0],ss@[10,9]
start_at@[45,0],ss@[23,4],ss@[47,0],ss@[23,3]

COLOR: Medium Purple,start_a_new_chain,9ch,turn
COLOR: Light Green,ch,sk,3ss,COLOR: Medium Purple,6ss,turn
COLOR: Medium Purple,ch,sk,6ss,COLOR: Light Green,3ss,turn
COLOR: Light Green,ch,sk,3ss,COLOR: Medium Purple,6ss,turn
COLOR: Medium Purple,ch,sk,6ss,COLOR: Light Green,3ss,turn
COLOR: Medium Purple,
start_at@[57,9],sc@[27,7],sc@[57,8],sc@[26,7],sc@[57,7],sc@[25,7],sc@[57,6],sc@[15,15],sc@[57,5],
sc@[14,15],sc@[57,4],sc@[13,15],sc@[57,3],sc@[12,15],sc@[57,2],sc@[11,15],sc@[57,1],sc@[10,15],sc
@[57,0]
start_at@[53,9],sc@[27,10],sc@[53,8],sc@[26,10],sc@[53,7],sc@[25,11],sc@[53,6],sc@[15,12],sc@[53,
5],sc@[14,12],sc@[53,4],sc@[13,12],sc@[53,3],sc@[12,12],sc@[53,2],sc@[11,12],sc@[53,1],sc@[10,12]
,sc@[53,0]
start_at@[54,9],ss@[10,14],ss@[57,0],ss@[10,15]
start_at@[54,0],ss@[27,10],ss@[56,0],ss@[27,8]

COLOR: Medium Purple,start_a_new_ch´ain,9ch,turn
COLOR: Light Green,ch,sk,3ss,COLOR: Medium Purple,6ss,turn
COLOR: Medium Purple,ch,sk,6ss,COLOR: Light Green,3ss,turn
COLOR: Light Green,ch,sk,3ss,COLOR: Medium Purple,6ss,turn
COLOR: Medium Purple,ch,sk,6ss,COLOR: Light Green,3ss,turn
COLOR: Medium
Purple,start_at@[66,9],ss@[31,7],ss@[66,8],ss@[30,7],ss@[66,7],ss@[29,7],ss@[66,6],ss@[15,18],ss@
[66,5],ss@[14,18],ss@[66,4],ss@[13,18],ss@[66,3],ss@[12,18],ss@[66,2],ss@[11,18],ss@[66,1],ss@[10
,18],ss@[66,0]
start_at@[62,9],ss@[31,9],ss@[62,8],ss@[30,9],ss@[62,7],ss@[29,9],ss@[62,6],ss@[15,16],ss@[62,5],
ss@[14,16],ss@[62,4],ss@[13,16],ss@[62,3],ss@[12,16],ss@[62,2],ss@[11,16],ss@[62,1],ss@[10,16],ss
@[62,0]
#start_at@[66,9],ss@[31,8],ss@[62,9],ss@[31,9]
#start_at@[66,0],ss@[10,18],ss@[64,0],ss@[10,17]

COLOR: Medium Purple,start_a_new_chain,9ch,turn
COLOR: Light Green,ch,sk,3ss,COLOR: Medium Purple,6ss,turn
COLOR: Medium Purple,ch,sk,6ss,COLOR: Light Green,3ss,turn
COLOR: Light Green,ch,sk,3ss,COLOR: Medium Purple,6ss,turn
COLOR: Medium
Purple,start_at@[69,9],ss@[33,7],ss@[69,8],ss@[33,7],ss@[69,7],ss@[7,38],ss@[69,6],ss@[6,31],ss@[
69,5],ss@[5,31],ss@[69,4],ss@[5,0],ss@[69,3],ss@[4,0],ss@[69,2],ss@[3,0],ss@[69,1],ss@[2,0],ss@[6
9,0]
start_at@[72,0],ss@[34,3],ss@[72,1],ss@[33,3],ss@[72,2],ss@[32,3],ss@[72,5],ss@[8,1],ss@[72,4],ss
@[7,1],ss@[72,5],ss@[6,1],ss@[72,6],ss@[5,1],ss@[72,7],ss@[4,1],ss@[72,8],ss@[3,1],ss@[72,9]
```

Inchworm-like:

Head and Tail:

```
BACKGROUND: White
COLOR: Steel Blue, 8ch,turn
sk,(hdc2inc,5hdc,hdc3inc).R,turn
COLOR: Medium Purple,(hdc@[0,1],4hdc,hdc2inc).R,ss@[0,-1]
ch,(hdc2inc,7hdc,hdc2inc,COLOR: Steel Blue,2hdc2inc,7hdc,hdc2inc)@R,hdc@[-1,-1],ss@[%,0]
ch,COLOR: Medium Purple,16ssbl,COLOR: Steel Blue,9ss,ss@[%,0]
[ch,sk,COLOR: Medium Purple,16ssbl,COLOR: Steel Blue,9ss,ss@[ch:%,0]
]*19
[ch,sk,COLOR: Light Green,16ssbl,COLOR: Steel Blue,9ss,ss@[ch:%,0]
]*16
[ch,sk,COLOR: Medium Purple,16ssbl,COLOR: Steel Blue,9ss,ss@[ch:%,0]
```

]*19
ch,sk,COLOR: Medium Purple,6ss,ss2tog,6ss,ss2tog,COLOR: Steel Blue,7ss,ss2tog,ss@[ch:%,0]
ch,sk,COLOR: Medium Purple,5ss,ss2tog,5ss,ss2tog,COLOR: Steel Blue,6ss,ss2tog,ss@[ch:%,0]
ch,sk,COLOR: Medium Purple,4ss,ss2tog,4ss,ss2tog,COLOR: Steel Blue,5ss,ss2tog,ss@[ch:%,0]
ch,sk,COLOR: Medium Purple,3ss,ss2tog,3ss,ss2tog,COLOR: Steel Blue,5ss,ss2tog,ss@[ch:%,0]
DOT: inflate=0.3

Body:

BACKGROUND: White
COLOR: Steel Blue, 8ch,turn
sk,(hdc2inc,5hdc,hdc3inc).R,turn
COLOR: Medium Purple,(hdc@[0,1],4hdc,hdc2inc).R,ss@[0,−1]
ch,(hdc2inc,7hdc,hdc2inc,COLOR: Steel Blue,2hdc2inc,7hdc,hdc2inc)@R,hdc@[−1,−1],ss@[%,0]
ch,COLOR: Medium Purple,16ssbl,COLOR: Steel Blue,9ss,ss@[%,0]
[ch,sk,COLOR: Medium Purple,6ssbl,COLOR: Light Green,4ssbl,COLOR: Medium Purple,6ssbl,COLOR: Steel Blue,9ss,ss@[ch:%,0]
]*50
ch,sk,COLOR: Medium Purple,6ss,ss2tog,6ss,ss2tog,COLOR: Steel Blue,7ss,ss2tog,ss@[ch:%,0]
ch,sk,COLOR: Medium Purple,5ss,ss2tog,5ss,ss2tog,COLOR: Steel Blue,6ss,ss2tog,ss@[ch:%,0]
ch,sk,COLOR: Medium Purple,4ss,ss2tog,4ss,ss2tog,COLOR: Steel Blue,5ss,ss2tog,ss@[ch:%,0]
ch,sk,COLOR: Medium Purple,3ss,ss2tog,3ss,ss2tog,COLOR: Steel Blue,5ss,ss2tog,ss@[ch:%,0]